Mechanical Hip Prosthetic

Conceptual Design Report

Aiden Camisa, Project Manager | CAD Lead
Quinn O'Neill, Website Designer | Machinist
Matt Martinez, Fundraising Lead | Anatomical & ANSYS Lead
Victoria Lyon, Budget Liaison | Anatomical Lead

Fall 2025-Spring 2026

Project Sponsor: NextStep Prosthetics
Faculty Advisor & Sponsor Mentor: Dr. Dante Archangeli, Dr. Reza Razavian
Instructor: Professor David Willy

DISCLAIMER

This report was prepared by students as part of a university course requirement. While considerable effort has been put into the project, it is not the work of licensed engineers and has not undergone the extensive verification that is common in the profession. The information, data, conclusions, and content of this report should not be relied on or utilized without thorough, independent testing and verification. University faculty members may have been associated with this project as advisors, sponsors, or course instructors, but as such they are not responsible for the accuracy of results or conclusions.

EXECUTIVE SUMMARY

This Mechanical Hip Prosthetic project aims to develop an active powered prosthetic hip designed to improve the lives of individuals who have undergone a hip disarticulation amputation. This device will allow users to drastically improve their quality of life by providing a more energy-efficient, stable, and supportive prosthesis. The project began in August 2025, led by a team of four mechanical engineering students. The team is guided by sponsors Dr. Dante Archangeli and Dr. Reza Razavian. The main objective is to create a powered prosthesis capable of fully supporting a 90 kg individual during walking, stair ascent and descent, as well as sitting and standing. The design will include a natural range of motion within the sagittal plane and compatibility with all standard types of prosthetic knees and sockets. To accomplish this, the team has partnered with Next Step Prosthetics and participated in the NSF I-Corps Aspire Program to gain valuable insights into user needs and functionality.

The current proposed design integrates multiple ideas generated by the team to create a simple and realistic prototype. This device utilizes a standard rotary motor to drive hip movement. To reduce weight, the design incorporates an industry-standard pylon to extend to the knee joint. The device has been refined through a detailed process involving mathematical modeling, SolidWorks design, and MATLAB analysis to create a prosthesis that benefits the user. The design targets motion within the sagittal plane from -20° to 130°, allowing for a natural gait pattern and smooth walking. The goal is for the device to operate for a minimum of 15 minutes before needing to recharge. The system will be controlled through a combination of motor controllers and sensors that automatically detect and determine when to lift.

Current progress within this design has included benchmarking, background research, and multiple rounds of concept selection and development. These steps allowed the team to break the design into multiple parts using functional decomposition and the black box method. Through these processes, the team identified four main subsystems: actuation, mechanism, power transmission, and attachment style. Mathematical modeling was then performed to determine the most effective options for each subsystem, leading to the final concept now in development.

This thorough design process has given the team confidence as they progress into prototype fabrication. The team is currently finalizing motor selection, motor control systems, and material choices. Multiple mathematical models were developed in MATLAB to compute torques for three potential motors: the AKE90-8 KV35, the AK60-39 V3.0 KV80, and the AK80-64 KV80. Additionally, the team identified aluminum, steel, 3D-printed polymers, and carbon fiber as promising materials for construction. A major design criterion is to make the prosthesis as light and simple as possible, improving usability for users and allowing for future development and refinement.

The next major step for the team is to begin prototype fabrication. This includes using PVC pipe to lay out the design, utilizing a Raspberry Pi and LabVIEW to control the motor and read sensor inputs, and maintaining an updated bill of materials and budget. According to the current schedule, the completed device is expected by Spring 2026.

TABLE OF CONTENTS

Contents

1 Background

Hip disarticulation amputations account for only 1% of all amputees, and yet it is one of the most debilitating. After such strenuous surgery, many individuals lose majority of their mobility and rely on solutions such as crutches, wheelchairs, or use current market available passive external hip prosthetics. As mentioned, there is only a limited range of passive hip joint prosthetics available, typically fashioned as a simple hinge fastened to a socket. However, these current models have been notably difficult to use and maneuver, causing users to expend significantly more energy in compensatory movement in gait. In creating an actively actuated hip joint, users will find more symmetry in gait, and the elimination of excess energy expenditure in mobility.

1.1 Project Description

The main goal of this project is to create an active hip prosthetic that allows amputees to experience the freedom of energy-efficient mobility again. Throughout the design process, our team has created and iterated over many various concepts in order to create the most practical solution. Each week, our team meets with our project clients to guide and inform design choices. In addition to our clients, we have also had unique opportunities to work with a local prosthesis clinic, Next Step Prosthetics. This collaborative opportunity has allowed us to speak directly to a hip disarticulation patient, as well as utilizing materials such as a genuine lower leg and knee joint prosthetics, and their facility 3D printing. Additionally, in our connection with NextStep Prosthetics has accounted for majority of fundraising through in-kind donations. Following the completion of the NSF I-Corps Aspire Course, we are currently waiting to learn if or when the funding will be available, as it was put on hold due to the previous government shutdown. However, with our allocated initial budget of $4,500 and in-kind donation, our team is still on track to remain within budget. Each of the factors mentioned above are continuously aiding the iterative design process of an active hip prosthetic.

1.2 Deliverables

The primary goal of designing, building, and testing an active powered hip prosthesis is to restore hip motion and eliminate excessive energy expenditure in prosthetic use for individuals who have lost their full leg during hip disarticulation. For this design, the baseline is to have a functional prototype that has active actuation with similar degrees of freedom to a normal leg. This should also be able to be controlled through some sort of control system that the user could control. As this is an upper leg prosthesis just for the hip, it must integrate with a standard prosthetic knee and a standard hip socket. In addition, it would need to be completed by a final report that includes the design specifications, control logic, safety documentation, and recommendations for continued development of the device. Regarding deliverables outside of the device itself, we are responsible for supplying funds outside of the further allocated amount, as well as keeping a detailed bill of materials and budget outlining fiscal aspects of the fabrication process. To assist in keeping us on schedule, a detailed Gantt Chart has been created in which class and client deliverables are included and sorted into various stages of progression. This project is also aiming to be a part of the NIH DEBUT Challenge for rehabilitative and assistive technologies, which includes additional deliverables to be carried out next semester, which could include items such as video demonstration, technical abstract, and supporting documents. The challenge guidelines have not yet been

confirmed, which we are anticipating in the spring of 2026.

1.3 Success Metrics

In measuring success for this project, there are many different categories in which we can divide. From a biomechanical standpoint, we measure success in the fluidity and efficiency provided from the design—how smooth and natural mobility is during use, as well as lifestyle integration factors, such as support and comfortability. Success in controls and electrical fields consists of programmed and intelligent components such as sensors, motor drivers, and electric efficiency and durability. Ensuring that the motor is successfully able to deliver the necessary power at certain times with minimal malfunction is ideally the goal for the active actuation of the design. Furthermore, mechanical success for this design would include gears capable of handling the imposed loads, shafts able to sustain torque transmission, appropriate bearing selections and installations, and structural integrity in the housing and bracket components.

Bringing each of these fields together, the design overall is aiming for active motion in the sagittal plane, a minimum continuous run time of 15-30 minutes, and must be load bearing of an individual up to 90 kg. Further, in material selection and durability, we aim to construct a system that is light as possible but allows users to comfortably put their weight onto it. We plan to test these by using a bypass method to measure and test the gait profiles of the device. We will also use engineering standards and FEA loads to ensure safety factors are achieved.

2 REQUIREMENTS

This chapter will include a listing of the requirements that the customers have for us as engineers. After the customer requirements were outlined, they were used to give us quantifiable engineering requirements. From those quantifiable requirements, we created a house of quality to best identify areas to prioritize throughout the design process.

2.1 Customer Requirements (CRs)

Our customer is a hip disarticulation patient who seeks to live a more active lifestyle than what is readily available to them with an unpowered hip prosthetic. These requirements include a stable leg, the ability to walk and climb stairs, easy and comfortable use, a non-cumbersome design, efficient battery life, and adaptable use. The stable leg implies the leg will be able to hold the weight of a 90kg user in standing and during all stages of the walking gate. The ability to walk and climb stairs implies that the leg will be able to reach a certain range of motion, and the motor will have enough power to allow the customer to ascend stairs. Both easy and non-cumbersome use highly depend on the shape and weight of our design, and is defined as how easy it is for the customer to lift, sit with, and perform everyday tasks with. Efficient battery life means the customer can use the leg throughout the day without a constant need to recharge. Adaptable use will mean that the leg can attach to most other lower leg prosthetics

2.2 Engineering Requirements (ERs)

With each customer requirement stated, we turn each of these goals into quantifiable goals, or at the very least, better define them within the scope of our project. To make the leg stable to stand and walk on, it will need to be able to regularly withstand the reaction force of walking and the stress that causes. We calculated the maximum stress to be around 64.854 MPa during the walking phase. Our goal for an easy, non-cumbersome design will be defined with a weight that is less than 20lbs and a sleek, intuitive design that does not inhibit any comfortability or movement. Additionally, the length of the system will be around 17in, close to the average upper leg length. For the range of motion, we determine that the hip joint should replicate a sound hip flexion and extension as closely as possible. This is quantified at about -20° in extension to 110° in flexion, with the assumption that 0° degrees is standing up straight. For the requirements of our motor, we need it to be able to lift the leg to around 110° from standing. The determined minimum torque for this motor will need to be 22Nm, assuming a gear ratio of 1 is used to transmit that torque to the leg. Additionally, it would need to be able to reach around .5 rev/s to match walking speeds. The exact battery used will depend on the completed design of the leg, but our goal will be an 8-hour battery life under regular usage.

2.3 House of Quality (HoQ)

Quality Function Deployment

Project title: Mechanical Hip Prosthetic
Team Members: Aiden Camisa, Victoria Lyon, Matthew Martinez, Quinn O'Neill
Date: Nov-5-25

Correlation:

+	.	-
Positive	No correlation	Negative

Relationships:

9	3	1	
Strong	Moderate	Weak	None

		Desired direction of improvement (↑,0,↓)	^		^	v					
	1: low, 5: high	Functional Requirements (How's) →	Motor that produces >22Nm of torque and speed of ~ 1m/s	100 degrees Range of Motion	Leg can handle 64.845 Mpa without buckling	Weight < 15 lbs	Control method allowing for personalized adjustment	Weighted Score	Competitive evaluation (1: low, 5: high) Satisfaction rating	Helix 3D by ottobock	Unpowered Hinged Femur
	Customer importance rating	Customer Requirements - (What's) ↓									
1	4	Ability to reliably lift leg to any resonably desireable height (stairs)	9	9	7	9	3	148	5	4	1
2	2	Natural/Comfortable gait	1	9	0	3	9	44	4	3	2
3	1	Comfortable shape/ fitting	3	1	7	7	0	18	5	5	3
5	5	Leg is can hold customer upright	0	1	9	0	0	50	5	5	3
6	3	Ability to use for enough time to complete disired activities (~ 1hr)	7	0	7	3	3	60	3	5	5
		Technical importance score	62	60	101	58	39	320			
		Importance %	19%	19%	32%	18%	12%	100%			
		Priorities rank	**2**	**3**	**1**	**4**	**5**				
		Difficulty	2	1	1	2	3	1: very easy, 5: very difficult			
		Cost and time	5	1	3	1	3	1: low, 5: high			
		Priority to improve	**2**	**3**	**5**	**1**	**4**				

Figure 1: Quality Function Deployment

Compiling each of the identified customer and engineering requirements, the Quality Function Deployment chart depicted in Figure 1 displays the scoring and importance of each interaction. As a result, ability to withstand buckling / structural integrity was identified as a major area of importance, followed by motor selection and ability. So far, we have satisfied motor requirements with our motor selection of the CubeMars AK80-64 KV80 robotic actuator, with rated torque of 42 N-m and maximum torque of 122 N-m [1].

3 Research Within Your Design Space

3.1 Benchmarking

Within the field of powered prosthesis, many different models exist for limbs and joints such as the knee, ankle, shoulder, and wrist. However, there are currently no powered hip prostheses available. Therefore, we selected the most technologically advanced passive hip prosthesis, as well as the baseline, most available model. Further, we include a generic subsystem adapter in our benchmarking process, as our product must be compatible with this system.

The Helix3D Hip Joint by Ottobock [2] is the most advanced system commercially available. Utilizing springs and hydraulics, the system is passively powered by movement and is advertised to create a more even and fluid gait. The system can support up to 100kg and is usable through 130° of motion in

the sagittal plane. This system is primarily made up of aluminum components.

Next, the most common type of hip prosthetic available resembles a simple hinge, known as a uniaxial hip prosthetic. While this product is not confined to a specific company, it is a common solution for those who experience hip disarticulation [3]. This model confines motion to the sagittal plane and does not include any kind of passive actuation or mechanism. This system is also able to support 100kg. Additionally, this model is also composed of aluminum.

Lastly, every prosthetic hip joint must have an adapter to connect to a knee joint. It is universally an unofficial standard to implement the use of a pyramid adapter [4]. Able to support up to 181kg and 12N-m of torque, the pyramid adapter is a universal subsystem in the field of prosthetics. The adapter is commonly made of titanium or, occasionally, stainless steel. Our team found it necessary to include this subsystem in our benchmarking to reinforce and ensure that our product will be compatible with the adapter design.

3.2 Literature Review

Each member of our team independently conducted a Literature Review to gain expertise in various topics spanning prosthetics and biomechanics.

3.2.1 Aiden Camisa

[3] “A normative database of hip and knee joint biomechanics during dynamic tasks using anatomical regression prediction methods” This article talks about the biomechanics of the hip and knee, which will assist in our design by looking at the angles of movement. The authors collected motion capture and force data from healthy adults to establish baseline joint angles, moments, and forces. They used statistical models to predict joint biomechanics based on anatomical parameters. The findings provide standardized data that can serve as a reference for prosthetic design and rehabilitation planning. This database helps clinicians and engineers identify deviations from typical joint mechanics in patients with limb loss or mobility impairments, which can further assist in informing our design.

[4] “GLOBAL STANDARDS FOR PROSTHETICS AND ORTHOTICS” ISO 7206-8: Endurance performance of stemmed femoral components under cyclic loading. This is a page based on the general standards of Prosthetics and Orthotics. It is useful to make sure we follow global standards for devices. This resource guides our team to ensure our prosthetic device meets rigorous performance and safety criteria. It is particularly relevant for hip disarticulation prostheses, where mechanical reliability and alignment are critical.

[3] “Hip biomechanics” This is a page that gives degrees of movement of the hip for all movement angles. The authors highlight how understanding hip mechanics is critical for surgical planning, rehabilitation, and prosthetic design. The paper discusses the kinematics of the hip during various activities, such as walking, running, and jumping. Understanding these biomechanical principles helps optimize gait patterns in amputees, which was identified as a critical aspect by Prosthetist Mentor Mike K.

[5] “Powered ankle-foot prosthesis” An example of a powered ankle prosthetic, we could use different aspects of a design for a different joint for the hip. The paper highlights improvements in energy efficiency and gait symmetry compared to passive prostheses. It also discusses the challenges of

designing robust and lightweight actuators suitable for daily use. Further, it also includes the importance of integrating sensors and control systems in a powered prosthetic.

[6] “The Design, Control, and Testing of an Integrated Electrohydrostatic Powered Ankle Prosthesis” Another example of an ankle prosthetic, however, utilizes an integrated electrohydrostatic actuation. The paper highlights the importance of precise torque control and real-time adaptability for gait restoration. The findings provide insight into integrating hydraulic and electronic components in lower-limb prostheses, which we have uncovered is no longer a viable option, as advised by our Sponsor Mentors.

[7] “A review of current state-of-the-art control methods for lower-limb powered prostheses” This is a review of different methods for controlling prostheses, particularly for lower-limb prostheses. The authors discuss the advantages and limitations of each method, focusing on robustness, responsiveness, and energy efficiency. They also highlight human-in-the-loop control strategies that improve gait symmetry and reduce user effort. As our team begins to explore control methods, this provides optimal introductory information.

[8] “Overview of Hip Disarticulation” A general overview of prostheses for Hip Disarticulation, which we found to be useful for comparing designs and revising work. The author specifically reviews socket designs, suspension methods, and joint mechanisms used in contemporary devices. The paper also discusses challenges faced by amputees, including stability, gait symmetry, and energy expenditure.

3.2.2 Victoria Lyon

[9] “Does the new Helix 3D hip joint improve walking of hip disarticulated amputees?” A study on comfort and usability for 3 patients, which we found offers insight for design improvements and preliminary preferences. In this study, participants underwent gait analysis before and after receiving the prosthesis. The study highlights the importance of multidirectional motion in restoring functional gait. It also provides empirical data supporting the effectiveness of innovative hip joint designs.

[10] “A pelvic kinematic approach for calculating hip angles for active hip disarticulation prosthesis control” An in-depth study providing useful information regarding sensors and control systems from the natural body kinematics. Using motion capture and sensor data, the authors developed algorithms to calculate real-time joint angles from pelvic motion. The method enables more accurate control of powered hip joints during swing and stance phases. The findings highlight the importance of integrating kinematic modeling into prosthetic control systems, as opposed to other types of control models.

[11] “Loads in hip disarticulation prostheses during normal daily use” A static assessment of the prosthetic leg and hip was helpful in mathematical modeling and general comprehension. The authors measured forces and moments during walking, sitting, and stair climbing in a cohort of patients. Findings indicate that prosthetic components are subjected to complex, multi-directional loads that must be considered in design. This was also helpful information to keep in mind for material and mechanism selection.

[12] "Design and prototype validation of a laterally mounted powered hip joint prosthesis" A Master's student thesis on a laterally mounted power hip, which opposed the common mounting style to the front of a socket. The authors conducted biomechanical tests to validate the range of motion, joint torque, and gait stability. The paper also highlights challenges in actuator integration and weight distribution, which we hope to learn from and integrate into our design thought process.

[13] "Energy expenditure during walking in amputees after disarticulation of the hip. A microprocessor-controlled swing-phase control knee versus a mechanically-controlled stance phase

control knee" This study is centered on comparing active knee prosthetics in standing or walking. The data collected measured oxygen consumption and gait parameters during treadmill walking. Results showed that microprocessor-controlled swing-phase knees significantly reduced energy expenditure and improved gait efficiency. The study highlights the advantages of integrating smart control technologies into prosthetic limbs, which we again hope to smoothly integrate into our design space as we begin to analyze

[14] "Biomechanical gait analysis for a hip disarticulation prosthesis: power source for the swing phase of a hip disarticulation prosthetic limb" In this study, the authors analyze where the body draws power to propel movement after hip disarticulation. The results are useful for improving gait symmetry and reducing compensatory movements, which we found to be a major component of patient dissatisfaction from our interview with an individual with Hip Disarticulation.

[15] "Design and optimization of a hip disarticulation prosthesis using the remote center of motion mechanism" The improvement of walking motion with a prosthetic utilizing the body's center of motion, which is additionally useful in suspension design choices and passive actuation. The authors modeled joint kinematics to reduce the lateral displacement of the prosthetic limb during walking. Testing from this study indicated smoother swing-phase motion and reduced energy expenditure with a remote center of motion.

[16] "Loading of Hip Measured by Hip Contact Forces at Different Speeds of Walking and Running" This study uses motion capture and musculoskeletal modeling to quantify hip contact forces during walking and running across a range of speeds. The authors found that hip forces rise significantly with increasing speed, and that running produces substantially higher loads than walking. They also show that muscle activity, especially hip adduction and extension moments, is a stronger predictor of hip loading than ground reaction forces alone. The research provides valuable insight into designing exercise programs aimed at stimulating osteogenesis or managing hip joint loading.

[17] "Development of a Powered Four-Bar Prosthetic Hip Joint Prototype" This article describes the design and initial testing of a powered four-bar linkage hip joint using optimization-based design, finite element analysis, and ISO-standard static compression tests. Walking trials with able-bodied participants wearing a prosthesis simulator to test kinematic feasibility were done.

[18] "An Investigation into a Gear-Based Knee Joint Designed for Lower Limb Prosthesis" This paper presents the design of a gear-based knee joint aimed at improving mechanical above-knee prostheses. Using gear design, material selection, and structural testing, the authors evaluate whether the joint can sustain loads typical for gait. They show that the gear-based joint design offers promising mechanical performance, suggesting that such a mechanism could enhance stability or functionality compared to conventional passive prosthetic knees. The work provides a valuable foundation for the trajectory of our current design.

[19] "Comparing the mechanical energetics of walking among individuals with unilateral transfemoral limb loss using socket and osseointegrated prosthetic interfaces" This study compares walking mechanics in eight individuals with unilateral transfemoral amputation before and 24 months after (osseointegrated, bone-anchored) prosthetic interface surgery. The findings highlight that while osseointegration may alter limb-level energetics, it does not necessarily redistribute work within the prosthetic joints; instead, energy losses previously absorbed by the socket may be transferred to the body's center of mass. This work contributes important biomechanical insight into how prosthesis interface type affects gait energetics and may inform prosthesis design or rehabilitation strategies post-osseointegration

3.2.3 Matt Martinez

[20] “Wearable Robotics: Challenges and Opportunities” A book spanning wearable robotics, including exoskeletons and powered prostheses. The author discusses engineering challenges such as actuation, control, and human-robot interaction. Case studies illustrate applications in rehabilitation and mobility restoration. The book also addresses opportunities for improving energy efficiency and adaptability in robotic devices, which we have taken into account with design and actuation.

[21] AGMA. “Standards & Emerging Technology American Gear Manufacturers Association (AGMA)” A technical standard with important implications, as our design potentially includes the use of a gearbox. The guidelines ensure durability, precision, and reliability, which are crucial for prosthetic joint mechanisms. It includes specifications for materials, load capacity, and tolerances.

[22] “Overview of the Components Used in Active and Passive Lower-Limb Prosthetic Devices” A chapter on the technical details of joints, actuators, and sockets to help guide our selection. The chapter also discusses material selection and design considerations, helping us to further understand integration challenges and trade-offs.

[23] “Total Hip Disarticulation Prosthesis with Suction Socket” A case report that offers practical challenges with sockets, which will help us design a prosthetic that is more socket-adaptable. The study highlights the role of socket fit and suspension in prosthetic performance, which remains relevant in our analysis to determine the best configuration to suspend the joint.

[24] “The biomechanics of trans-femoral amputation” Important and helps to understand load transfer, gait mechanics, and biomechanical limitations in above-the-knee amputations (hip disarticulations). Findings inform alignment, socket design, and joint selection in prostheses, and by understanding mechanical stresses, we can help prevent overuse injuries and improve mobility.

[25] "A multiple-task gait analysis approach: Kinematic, kinetic, and EMG reference data for healthy young and adult subjects A study that provides a baseline for gait and force data on healthy subjects. It supports the design of prostheses that restore natural movement patterns. The dataset is particularly useful for validating powered hip and knee devices. In turn, this can also be used to compare against prosthetic gait data to evaluate function quality.

[26] "State of the Art and Future Directions for Lower Limb Robotic Exoskeletons” Highlights current trends and limitations in robotic exoskeletons, which can inform various aspects of our prosthetic design, such as power, weight, and comfort.

3.2.4 Quinn O’Neill

[27] “EMG Muscle Activation Pattern of Four Lower Extremity Muscles during Stair Climbing, Motor Imagery, and Robot-Assisted Stepping: A Cross-Sectional Study in Healthy Individuals” This study investigates control strategies for powered transfemoral prostheses during stair ascent. The authors designed and tested algorithms that coordinate knee and hip actuation based on real time sensor feedback.

[_28] “On the design evolution of hip implants: A review” Study on hip implants, detailing materials and systems best used to replace a hip. This will allow us a basic idea of how to best connect our prosthetic to the hip of a patient. The findings highlight the growing demand for advanced prosthetic technologies. Understanding population trends supports innovation in high-performance prostheses.

[29] “A novel hip joint prosthesis with uni-directional articulations for reduced wear” The unidirectional hip articulator is the most basic benchmark, as examined in the benchmarking sections.

[30] "Ground reaction forces at different speeds of human walking and running" This paper examines the biomechanics of gait in individuals with and without prosthetic limbs using ground reaction force analysis. The authors identify characteristic differences in loading, propulsion, and balance between the two groups.

[31] "Shijiazhuang Perfect Prosthetic Manufacture Co., Ltd." The upper-to-lower leg pyramid adapter, a common adapter found on lower limb prosthetics, is a good benchmark for designing the lower attachment for our prosthetic, as mentioned in the benchmark.

[32] "(PDF) A review of gait cycle and its parameters" An analysis of the stages of the walking gait cycle, in which subjects demonstrate how a bionic ankle–foot prosthesis can restore near-normal walking biomechanics. The authors used a powered system comparable to biological muscles. Results showed improved gait symmetry, reduced metabolic cost, and enhanced walking speed.

3.3 Mathematical Modeling

3.3.1 Torque Analysis for Hip Flexion – Matt Martinez

To estimate the torque required for hip flexion, the leg was modeled as a rigid body subjected to gravitational loading and joint geometry constraints. Two equations were used to describe the static torque at the hip:

$$\tau = rFsin\theta \tag{1}$$

Where τ is the joint torque (N·m), F is the applied muscle or actuator force (N), and r is the effective moment arm length (m).

The static torque on the hip was then modeled as:

$$\tau_{hip}(\theta, \beta) = m_{thigh}gr_{thigh}sin\theta + m_{shank}g(L_1 sin\theta + r_{shank}\sin(\theta - \beta)) + m_{foot}g(L_1 sin\theta + L_2 \sin(\theta - \beta)) \tag{2}$$

Where m is the mass (kg), g is gravitational acceleration (9.81 m/s²), L is the length (m), θ is the hip flexion angle (°), β is the knee flexion angle (°), and r is the center of mass (m)

These equations were used to calculate the torque required to lift the leg at various knee flexion angles (0, 60, 90), where the hip angle is 90. The plot shows that static hip torque decreases from 58.3 N·m at 0° knee flexion to 45.8 N·m at 90°. MATLAB was used for data processing and curve generation

3.3.2 Power and Battery Analysis – Aiden Camisa

This analysis outlines the electrical power and battery sizing requirements for an active hip prosthetic. Mathematical modeling using sinusoidal approximations for hip motion and torque interpolations helps to set requirements for the battery. Equations necessary are:

$$\theta(t) = \theta_0 + Asin\left(\frac{2\pi t}{T}\right) \tag{3}$$

$$\omega(t) = \frac{d\theta}{dt} = A \cdot \frac{2\pi}{T}\cos\left(\frac{2\pi t}{T}\right) \tag{4}$$

$$E = \int_0^T \frac{\max(Pmech(t),0)}{\eta_{motor}} dt + P \cdot T \tag{5}$$

Where $\theta(t)$ is the angle with respect to time, θ_0 is the initial angle, $\omega(t)$ is the angular velocity (rad/s), P_{mech} is the mechanical power (W), and E_{step} is the electrical energy per step. The results are in the table below:

Time (Min)	Battery required (Wh)
10	21.73
20	43.46
30	65.19
45	97.79
60	130.38
90	195.57

Table 1: Battery Sizing for Active Hip Prosthetic

3.3.3 *Forces on Leg Due to Walking – Quinn O'Niell*

This analysis provides critical insights into the peak loads experienced by the leg during normal walking. Reaction force is approximately 1.5 times body weight during heel strike/toe-off, and body weight at mid-stance for a 90 kg mass. – Foot length: 24.16 cm, shank length: 39 cm, foot at 90° to shank, heel/toes at 20° to ground. Reaction forces are modeled by:

$$R_1 = 1.5mg \tag{6}$$

$$R_2 = mg \tag{7}$$

R_1 is the reaction force during heel strike and toe-off (N), R_2 is the reaction force at mid-stance (N), m is the mass of the individual (kg), and g is gravitational acceleration (9.81 m/s²). A static equilibrium analysis is then performed to determine force and moment distributions and a geometric modeling of leg segments during gait phases (heel strike, mid-stance, toe-off):

$$\sum F = 0 \tag{8}$$

$$\sum M_k = 0 \tag{9}$$

where ΣF is the sum of forces (N) and ΣM_k is the sum of moments about the knee (Nm).

$$F_t = F_k \sin\theta$$

(10)

$$F_a = F_k \cos\theta$$

(11)

F_t is the transverse force (N), F_a is the axial force (N), F_k is the force at the knee (N), and θ is the angle of the force (degrees). - Maximum force: 1.324 kN during heel strike and toe-off

The maximum force of 1.324 kN and moment of 176.65 kNm highlight the need for robust materials and designs capable of withstanding these dynamic loads.

3.3.4 Stress and Strain on a Prosthetic Leg – Victoria Lyon

This is a stress-strain analysis using material properties (Young's modulus), as well as load distribution modeling for standing and walking scenarios, aiding in material selection. Equations used include:

$$\sigma_{axial} = \frac{F}{A} \quad (12)$$

$$\sigma_{bending} = \frac{Mc}{I} \quad (13)$$

$$\varepsilon = \frac{\sigma_{max}}{E} \quad (14)$$

Where σ_{axial} is axial stress (MPa), F is the applied force (N), A is the cross-sectional area (m^2), $\sigma_{bending}$ is bending stress (MPa), M is moment (Nm), c is distance from neutral axis to outer fiber (m), I is moment of inertia (kgm^2), ϵ is strain, σ_{max} is maximum stress (MPa), and E is Young's modulus (MPa).

While standing $\sigma_{axial} = 5.0185$ MPa, $\epsilon = 7.169(10^{-5})$. While walking $\sigma_{axial} = 7.528$ MPa, $\sigma_{bending} = 57.317$ MPa, $\sigma_{max} = 64.845$ MPa, and $\epsilon = 0.0009262$. The stress and strain calculations reveal that walking imposes significantly higher bending stresses compared to standing, with maximum stress reaching 64.845 MPa. This underscores the importance of using high-strength materials like aluminum with appropriate thickness.

3.3.5 Static Force Analysis on Attachments – Aiden Camisa

The static analysis compares various attachment configurations, showing that dual attachments minimize stress concentrations. Static force and moment equilibrium equations are used:

$$F = mg \quad (15)$$

$$M = Fd \quad (16)$$

Where F is the total force (N), m is the mass (kg), g is gravity (9.81 m/s^2), M is the moment (Nm), and d is the distance between bolts (m). Below is the free-body diagram that was used:

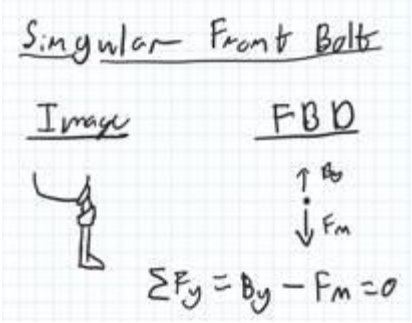

Figure 2: Free-body Diagram of Prosthetic

Then the force is used to find the force per bolt (F_b) and shear stress (σ_{shear}):

$$F_b = \frac{F}{n} \tag{17}$$

$$\sigma_{shear} = \frac{F_b}{A} \tag{18}$$

Shear stress is in MPa, force per bolt is in N, n is the number of bolts, and A is the area (m^2). The table below shows the different attachment used and their respective values.

Type	Force (N)	Moment (N*m)	Force per Bolt (N)	Bearing Stress (MPa)	Shear Stress in the bolt (MPa)
Dual Attachment	882.90	52.974	441.45	13.80	8.78
Laterally Mounted	882.90	70.632	882.90	27.59	17.56
Singular Front Bolt	882.90	88.29	882.90	27.59	17.56
Angled Corner	882.90	105.948	882.90	27.59	17.56

Table 2: Comparison of Attachment Designs

The lowest shear stress of 8.78 MPa in dual setups enhances structural integrity and is optimal for load distribution, reducing failure risk and improving prosthetic stability under body weight loading.

3.3.6 Actuation Static Force Analysis – Quinn O'Neill

This analysis determines the force needed for actuators to achieve a 100° hip motion

range by using moment and force balances for selecting actuators (hydraulic, pneumatic, and electronic linear). The equations that model this are equations (8),(9), (15), and (16). Center of mass (COM) percentages are 43% for the thigh, 43% the shank, and 42% for the foot. The results yield a required actuator force of 142.8 N for a 42.854 Nm moment.

The 142.8 N requirement allows selection from various actuator types, with cost as a deciding factor. All three actuator types (hydraulic, pneumatic, electronic) are viable, but the cheapest reliable option should be chosen for cost-effective design without compromising performance.

3.3.7 Joint and Motor – Matt Martinez

The joint and motor analysis models human hip motion to select appropriate motors and gearing. The torque of the hip) is given from a data set, and then body weight (BW) is factored in.

$$\tau_{hip} = -BW \cdot \tau \tag{19}$$

Other variables calculated for the hip joint are angular velocity (ω_{hip}) in rad/s and power (P_{hip}) in watts. θ is the hip angle in degrees.

$$\omega_{hip} = \frac{d\theta}{dt} \tag{20}$$

$$P_{hip} = \tau_{hip} \cdot \omega_{hip} \tag{21}$$

Results were calculated and then modeled using MATLAB. Below are the kinematics at the hip joint during normal gait over one cycle (1.2 seconds):

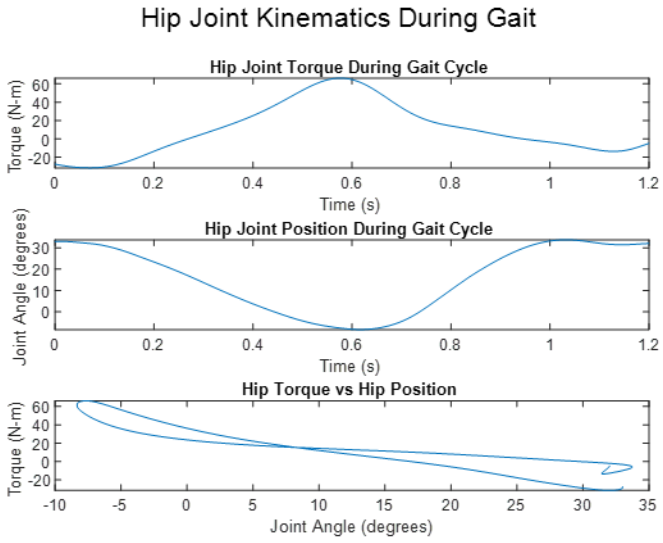

Figure 3: Hip Joint Kinematics During Gait Cycle

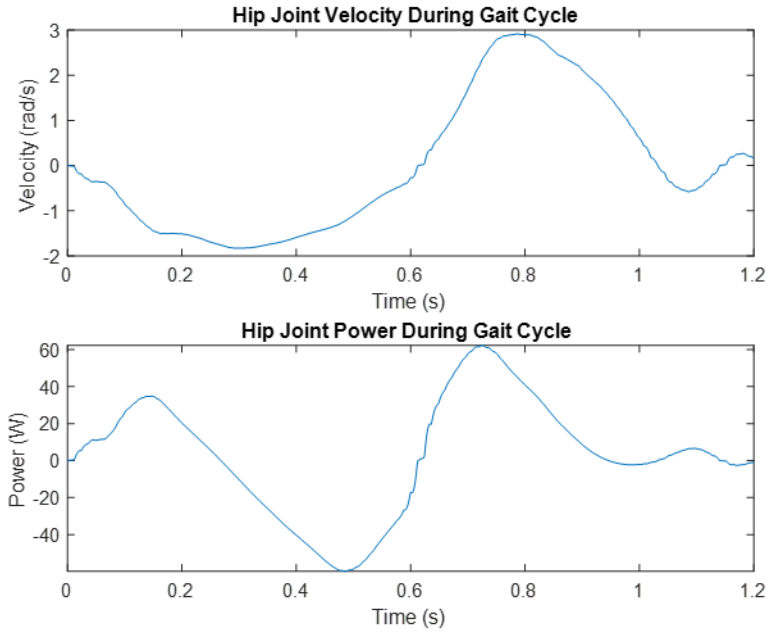

Figure 4: Hip Joint Velocity and Power During Gait Cycle

Next, the specifications from the chosen motor are used to find the current (I) in amps, voltage (V) in volts, and power (P) in watts.

$$I = \frac{\tau_m}{k_t} \tag{22}$$

$$V = IR + k_t \omega_m \tag{23}$$

$$P = V \cdot I \tag{24}$$

τ_m is motor torque (Nm), k_t is the torque constant (Nm/A), R is resistance (Ω), and ω_m is the motor angular velocity (rad/s). The following graphs show these models:

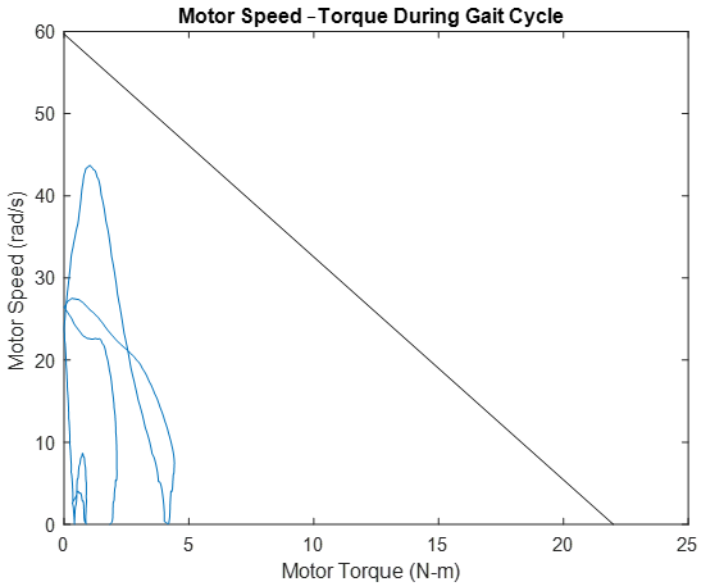

Figure 5: Motor Speed-Torque During Gait

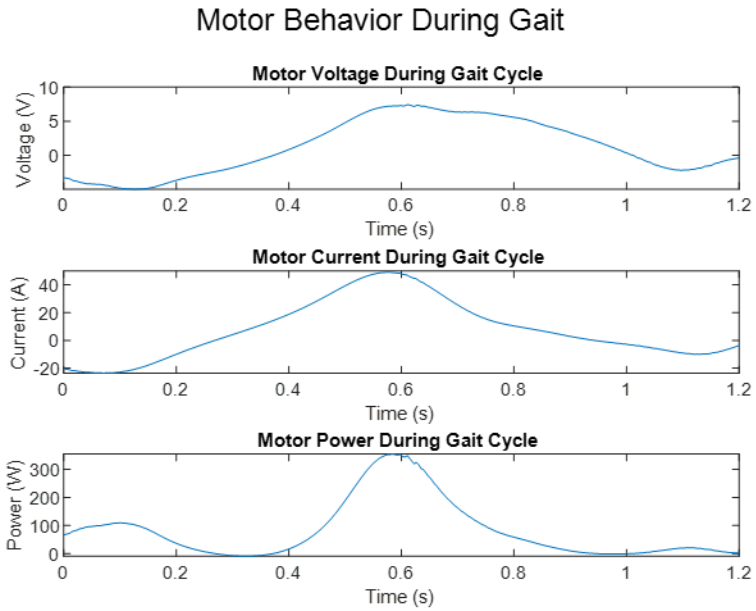

Figure 6: Motor Behavior During Gait

The AK80-9 motor meets torque and power needs, but high gear ratios increase inefficiency.

3.3.8 Preliminary Shaft Material Evaluation – Victoria Lyon

To transmit torque from the motor, a flanged shaft must be mounted directly to the CubeMars motor. Thus, a shaft must be designed to properly transmit oscillations and handle the loads that will be incurred in use. To begin, initial assumptions were defined as:

- $d = 20mm$
- $T_m = 48\ N * m$
- $M_a = 176\ kN * m$
- $S_e(AL) = 270\ MPa \mid S_{ut}(AL) = 110\ MPa$
- $S_e(Ti) = 480\ MPa \mid S_{ut}(Ti) = 550\ MPa$
- $T_a = M_m = 0$

These parameters were then used to compute von Mises stresses of two different materials to check for static failure:

$$\sigma'_a = \sqrt{\left(\frac{32K_f M_a}{\pi d^3}\right)^2 + 3\left(\frac{32K_{fs}T_a}{\pi d^3}\right)^2} \quad (25)$$

$$\sigma'_m = \sqrt{\left(\frac{32K_f M_m}{\pi d^3}\right)^2 + 3\left(\frac{32K_{fs}T_m}{\pi d^3}\right)^2} \quad (26)$$

In which the results are listed in the table below:

Results	Aluminum (6061)	Titanium (Grade 4)
σ'_a	336.25 MPa	340.71 MPa
σ'_m	.0382 MPa	.0425 MPa
σ'_{max}	336.29 MPa	340.75 MPa

Table 3: von Mises Stress Calculations for Potential Shaft Materials

4 Design Concepts

4.1 Functional Decomposition

Component	1	2	3	4
Actuation	Electronic Linear actuator	Series Elastic Actuators	Rotary Actuator	Variable Stiffness Actuator
Power Transmission	Gear system	Cable	Electrostatic clutch	Belt
Mechanisms	Stewart platform with 2 Links	Ball Joint	Universal Joint	Rigid Links

Suspension / Attachment Configuration	Dual attachment [2 components bolted to the socket]	Lateral [side socket attachment]	Singular front bolt [typical use]	Angled alignment [lower corner attachment,

Table 4: Functional Decomposition Table

This is a chart detailing each of our important criteria for function, and 4 different possibilities for each criterion. Our first criterion is actuation, a means to extend and contract parts of the leg to best fit the movement of the walking cycle. Next is Power transmission, which is how we will get the motor to connect to and power the movement of the leg. Third is mechanisms, which are means to connect each component of the leg and still allow for freedom of movement within our specified range. Finally, our method of attaching the leg to the prosthetic cast.

4.2 Concept Generation

Concepts were not individually drawn, but were all understood by each team member.

For means of actuation, we found that the hydraulic was the strongest but most expensive, and the electronic linear actuator was the weakest and cheapest. Therefore, under guidance and recommendation from our clients, rotary robotic motors were a viable option and most accessible for our application. After lots of different research and analysis, our team was able to select a motor that successfully meets and exceeds the necessary force and torque parameters for the prosthetic.

As for power transmission, we opted for a compact and durable system, in which gears were selected and designed for the application. Based on our own experience and knowledge, we felt most confident in designing and selecting a gearset that is capable of handling the variable loading conditions and transmitting the torque effectively.

Lastly, for means of suspension, the lateral side socket is closest to the sagittal center of rotation but is awkward to walk around on as it is loaded to the side of where a sound leg would be. The lower corner would technically be the most structurally sound for loading the leg when standing but would hinder the range of motion and also be difficult to sit with. Both the front and dual attachments allow for full range of motion in regard to the sagittal plane and further enable ease of installment for professionals.

4.3 Selection Criteria

To evaluate the design concepts, we as a team established criteria that we found would be impactful for our design. This included the performance needs, consistency needs, and practicality of our design. The primary criteria included structural safety, manufacturability, cost of device, and the device reliability and interface. Structural safety was important to make sure that our design could withstand the expected loading while avoiding failure within the device. Manufacturability allows us to consider how feasible the device would be for prototyping, and the final device. The cost of device is important as keeping it available to as many people as possible is important as well. Reliability is important as making sure the device would not fail in critical situations, or under different circumstances will allow us to prevent accidents that could happen within our device. Further, we have learned through the process to

additionally evaluate designs based on user experience and practicality, trying to address criteria such as body uniformity (protrusions/ unnatural look and feel).

4.4 Concept Selection

Moving forward to selecting components for comprehensive design, our team decided not to utilize a chart or scoring system but instead participated in an in-depth team-client discussion. This method allowed our team to present thoughts, mathematical analyses, and literature reviews for insight and feedback from our clients, who have experience and expertise in many of the components to be designed.

Our final design decisions were mindful of cost, implementation, and took our client's recommendations into account. To provide power, the CubeMars AK80-64 KV80 motor was selected based on its compact size, rated torque, and gear ratio of 64:1. To actually transmit the motor's power, gears were chosen for their durability, manufacturable advantage, and customizability. Using gears allows our team some room to further change or tweak aspects of the design, such as speed or gear strength. There were no further mechanisms chosen to be used in the design for the sake of simplicity and ease of use and assembly. Lastly, to suspend the hip joint to the socket interface, a dual attachment fastened above and below the joint provide the most security and strength for the design to soundly remain on the socket interface. While not explicitly depicted in concept generation, it is worthwhile to note that many components are to be manufactured from an aluminum alloy that is typically used in prosthetics, while others are to be mild steel materials.

5 Schedule and Budget

5.1 Schedule

5.1.1 First Semester Gantt Chart

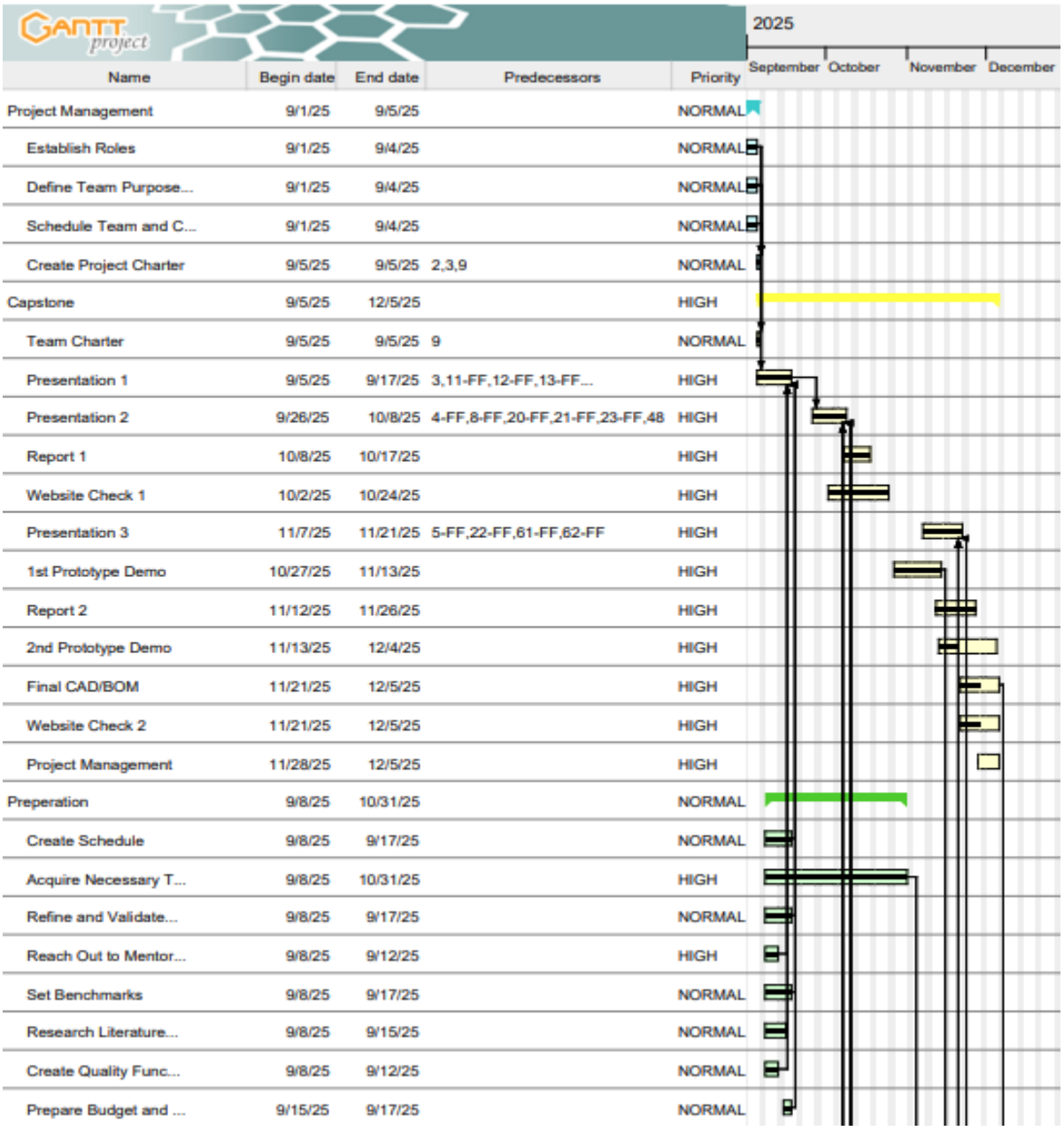

Name	Begin date	End date	Predecessors	Priority
Project Management	9/1/25	9/5/25		NORMAL
Establish Roles	9/1/25	9/4/25		NORMAL
Define Team Purpose...	9/1/25	9/4/25		NORMAL
Schedule Team and C...	9/1/25	9/4/25		NORMAL
Create Project Charter	9/5/25	9/5/25	2,3,9	NORMAL
Capstone	9/5/25	12/5/25		HIGH
Team Charter	9/5/25	9/5/25	9	NORMAL
Presentation 1	9/5/25	9/17/25	3,11-FF,12-FF,13-FF...	HIGH
Presentation 2	9/26/25	10/8/25	4-FF,8-FF,20-FF,21-FF,23-FF,48	HIGH
Report 1	10/8/25	10/17/25		HIGH
Website Check 1	10/2/25	10/24/25		HIGH
Presentation 3	11/7/25	11/21/25	5-FF,22-FF,61-FF,62-FF	HIGH
1st Prototype Demo	10/27/25	11/13/25		HIGH
Report 2	11/12/25	11/26/25		HIGH
2nd Prototype Demo	11/13/25	12/4/25		HIGH
Final CAD/BOM	11/21/25	12/5/25		HIGH
Website Check 2	11/21/25	12/5/25		HIGH
Project Management	11/28/25	12/5/25		HIGH
Preperation	9/8/25	10/31/25		NORMAL
Create Schedule	9/8/25	9/17/25		NORMAL
Acquire Necessary T...	9/8/25	10/31/25		HIGH
Refine and Validate...	9/8/25	9/17/25		NORMAL
Reach Out to Mentor...	9/8/25	9/12/25		HIGH
Set Benchmarks	9/8/25	9/17/25		NORMAL
Research Literature...	9/8/25	9/15/25		NORMAL
Create Quality Func...	9/8/25	9/12/25		NORMAL
Prepare Budget and ...	9/15/25	9/17/25		NORMAL

Image 1: First Semester Gantt Chart Part 1

Design	9/26/25	11/21/25		NORMAL
Create Functional D...	9/26/25	10/2/25		NORMAL
Perform Concept Gen...	9/26/25	10/6/25		NORMAL
Update Engineering Calculations	9/26/25	10/8/25		NORMAL
Evaluate Specifications	9/26/25	10/8/25		NORMAL
Create Initial CAD Assembly	10/6/25	10/8/25		NORMAL
Update Design Requirements	10/20/25	10/30/25		NORMAL
Define BOM and Perf...	10/22/25	10/23/25		NORMAL
Dimension Drawings ...	10/20/25	11/5/25		NORMAL
Perform Design FMEA	10/22/25	11/5/25		NORMAL
Create Design Descriptions	10/23/25	11/5/25		NORMAL
Perform FEA	10/10/25	11/21/25		NORMAL
Prototyping	10/24/25	11/24/25		NORMAL
Order Materials and Components	10/24/25	10/24/25	6	HIGH
Design Load-bearing Frame	11/3/25	11/12/25	17	NORMAL
Make As-needed Desi...	11/13/25	11/24/25		NORMAL
Design Socket Connection	11/3/25	11/12/25		NORMAL
Assemble Parts	11/10/25	11/12/25		NORMAL
Create and Demonstr...	11/13/25	11/13/25	54-FF	NORMAL
Testing	11/14/25	11/21/25	25	NORMAL
Define FOS and Testing Protocol	11/14/25	11/21/25		NORMAL
Documentation	10/6/25	1/15/26		NORMAL
Maintain a Design N...	10/6/25	12/5/25	4-SS,56-FF	NORMAL
Create End-of-Semes...	12/1/25	12/5/25		NORMAL
Prepare Summary and...	12/1/25	12/5/25		NORMAL
Create Beginning-of...	12/8/25	1/15/26	41	NORMAL
NIH DEBUT Challenge	3/24/26	8/25/26		NORMAL
Submissions Open	3/24/26	6/18/26		HIGHEST
Judging Period	6/22/26	8/18/26		HIGHEST
Winners Announced	8/25/26	8/25/26		HIGHEST

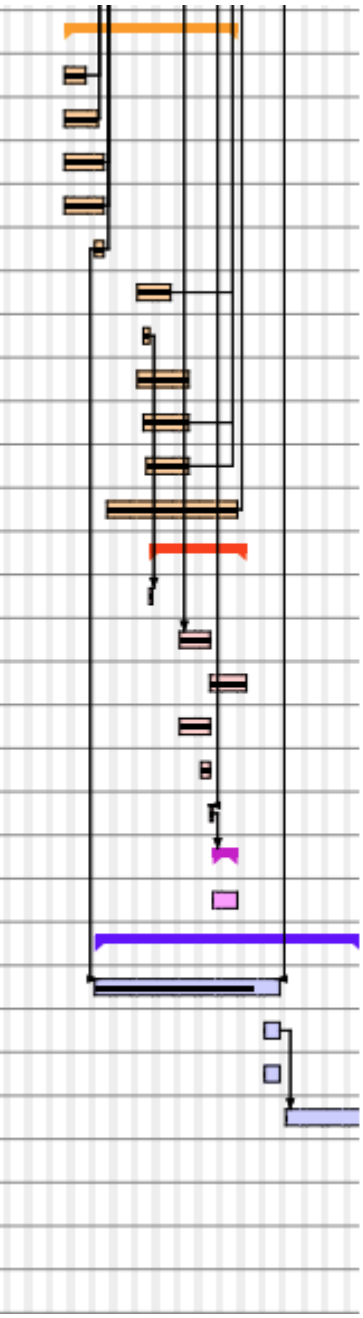

Image 2: First Semester Gantt Chart Part 2

5.1.2 Second Semester Work Breakdown Structure

UGRADS Requirements
• Registration
• Practice Presentation
• Symposium Presentation

Mechanical Engineering Development
• CAD updates and subsystem modeling
• Final CAD Packet

Electrical & Software Development
• Raspberry Pi control design
• Control demo
• Integration with actuators & sensors

Build Milestones
• 33% Build
• 67% Build
• 100% Build

Prototype Assembly
• Mechanical assembly
• Electronics integration
• Full system integration

Test Plan Development
• Initial Testing Results
• Product Demo & Final Testing Results

Poster & Presentation
• Draft Poster
• Final Poster & PPT
• Practice Presentations
• Symposium Presentation

Final Deliverables
• Final Report
• Final Website Check
• Spec Sheet
• Operation/Assembly Manual
• Client Handoff Package

5.2 Budget

Our team received an initial investment of $4,500 to fabricate and machine our active hip prosthetic design. So far, we have received many in-kind purchases from our mentors at NextStep, which has been extremely helpful in both application and budget consensus, allowing our team access to genuine prosthetic material and modern 3D printing technology. Further, we are currently still waiting to hear updates back on NSF I-Core Aspire course funding allocation, as it is unclear if or when the funds will be available. A total of $1,065.43 has been spent so far on material, majority of which is due to the motor cost of $911.77. We plan to continue fundraising efforts to ensure that our team will be able to purchase any necessary materials or manage any unforeseen monetary circumstances.

Budget Overview				
Budget		4500		
Fundraising		1550		
Expenses		1065.43		
Available Balance		4984.57		

FUNDRAISING LOG

Date	Source	Amount ($)	Type	Notes
Pending	i-Corp Aspire Course	$3,000	Monetary	On hold, not included
10/29/2025	NextStep Prosthetics	$1,500	In-Kind	Physical Lower Leg
11/5/2025	NextStep Prosthetics	$50	In-Kind	3D Printing

EXPENSE LOG

Date	Item/Purpose	Amount ($)	Location	Notes
10/27/2025	Adapter	$ 3.21	NAU Surplus	
10/27/2025	Micro HDMI cable	$ 31.81	BestBuy	
11/14/2025	AK80-64 Kv80 Motor	$ 911.77	CubeMars	With driver board. Discount code
11/14/2025	RUBIK Link V2.0	$ 40	CubeMars	Discount code
11/18/2025	CAN Bus HAT	$ 39.99	Waveshare	
11/25/2025	36V Battery	$ 32.83	Amazon	
11/26/2025	Battery Adapter	$ 5.82	Amazon	

Table 5: Current Budget Overview

5.3 Bill of Materials (BoM)

So far, 7 items have been purchased for the building and testing of our design, particularly for the electrical components. Materials and parts to be machined will likely be purchased at the beginning of next semester, as our team continues to analyze and iterate on design aspects. Further, as part of prototyping during this semester, 3D printing has been a main source of material for testing, donated in-kind by NextStep, as depicted in the budget above. The current bill of materials allocates parts that have

been purchased, again as further analysis is required to specify material and manufacturing for further components:

Hip Prosthetic Bill of Materials				
Item No.	**Description**	**Vendor**	**Unit Price**	**Purchase Date**
1	AK80-64 KV80 Motor	CubeMars	$911.77	14-Nov
2	RUBIK Link V2.0	CubeMars	$40	14-Nov
3	CAN Bus HAT	Waveshare	$39.99	18-Nov
4	36V Battery	Amazon	$32.83	25-Nov
5	Battery Adapter	Amazon	$5.82	26-Nov
6	Adapter	NAU Surplus	$3.21	27-Oct
7	Micro HDMI cable	BestBuy	$31.81	27-Oct

Table 6: Current Bill of Materials

6 Design Validation and Initial Prototyping

6.1 Failure Modes and Effects Analysis (FMEA)

1. Identify				2. Classify									3. Take action	4. Action results			
Item (component, part, assembly)	Function	Requirements	Failure mode	Effect(s) of potential failure	**Severity**	**Classification**	Potential causes of failure	Current design controls (prevention)	**Occurrence likelihood**	Current design controls (detection)	**Effectiveness of best method of detection control**	**RPN (Risk priority no.)**	Recommended action(s)	**Severity**	**Occurrence**	**Detection**	**RPN (Risk priority no.)**
Motor	Providing torque to the shaft	Motor must provide enough torque, smooth, accurate torque/positioning	Control instability or sustained vibration during gait	User discomfort, reduced balance, risk of fall, joint wear	9	Safety	Poor control tuning, insufficient damping	Torque limits, firmware control	3	Manual Testing, Encoder	3	81	Implement rate limits, use high-rate inner current/torque loop	9	2	2	36
Motor	Providing torque to the shaft	Motor must provide enough torque	Motor can not meet required torque to lift leg	Leg stops moving	4	Product failure	Motor is defunct	Product testing, inspection	1	Torque monitor, current sensing	1	4	Maintenance schedule	5	4	3	60

Motor Shaft	Power Transmission	Transmit movement	Detaches from motor	Hinders rotation	10	Safety	Fastener failure, vibration	Motor casing, using standard bolts	3	Gait stability	4	120	Include repair kit, include fasteners or clamps with design.	10	2	2	40
Motor Shaft	Power Transmission	Handles load	Shaft breaks	Joint & leg detaches	10	Safety	Material failure	Material Selection, mathematical modeling	2	Gait stability	4	80	Replace shaft, bring to prosthetist	5	3	3	45
Battery	Provide Power to the motor	Provides enough power for the motor to allow it to produce the required torque	Does not reach required power	The motor doesn't power the leg, and the leg is not able to reach the required gate	4	Product failure	Dysfunctional battery. Low power battery.	Mathematically determines the amout of power required for the motor	1	Low voltage alarm in testing	1	4	Use battery with 20-30% capacity margin	5	4	3	60
Battery	Provide Power to the motor	Provides enough power for the motor to allow it to produce the required torque	Wires break / detatch from motor	Leg stops moving with power. potential danger with loose wires	6	Safety	wires not secured tightly	Clips built into motor, and no major movement of motor or battery, and sealing of the wires to the mold	3	Motor stops working, look at wire	2	36	secure wires closely to the mold to prevent damage and movement	7	3	2	36
Rasberry Pi Controllor (Electrical system)	Acts as a computer to provide control	Simple and easy Interface	No Control of leg	Locks in place or becomes frozen in place. Possible triping and injury	4	Product failure	Code is wrong or something is unpluggedx	Rasberry pie with a CANbus attachment to the motor.	4	Testing the code and wiring before using it on a individual	5	80	Implement a test sequence to make sure everything works.	4	4	1	16
Attachment Plate	Suspend system on socket	Securely hold system without movement	Detaches from socket	System detaches	10	Safety	Extreme wear, unforseen force	Secure standard fasteners	2	Stability, inspection	3	60	Safety test, user manual	5	4	3	60

Table 7: FMEA of Hip Prosthetic

Above we can see our team's FMEA, which we used to narrow down critical potential failures. Some of the biggest potential failures that we could find are the raspberry pie microcontroller and the motor shaft of the gear train. Here we see that if the motor shaft were to fail then we could see this part of the system disconnecting or breaking from the stress and strain caused by forces and torque of the shaft

and the hip structure rotating. Since our leg only has movement within one direction of axis, we found that this could become an issue as its used more and more. As for the raspberry pie and electrical system failing, we know that our leg is one where the motor would be powered while it is worn. This means that if our motor ever didn't have the controls telling it what to do it could possibly collapse and be left immobile. As the whole point of our leg is to help make it easier to move around, the possibility that someone could be stuck somewhere or fall and hit their head is a huge critical failure point.

As for ways we are reducing the likelihood and chance of any of these failures happening, is by first the motor shaft. To assist in the critical failure point of the motor shaft we plan to implement a couple changes to help mitigate any harm. The first thing we will be doing is we will be performing multiple tests on the motor shaft to test the strength and weaknesses of our designs. In addition we will be using end clamps to lock the shaft in place vs. having the shaft just sit within the bearing holes. In addition, we will also include a repair kit that could be used to tune up and keep in good conation the different parts of the leg such as the shaft. This will assist in our critical failure point and it can be seen as before the mitigation we found that it would be 120 points which is very risky to now only 40 points. This shows that our risk trade off analysis is decreasing and our mitigation strategies is working.

Our other critical point was the possibility of the raspberry pie system not working or the electrical system possibly failing as well. A couple of our strategies to mitigate the effects of this failure that we will be implementing is, to implement a test start up code within our code to make sure that everything is connected and working before even attaching to the socket. In addition we will also try to mitigate this by leaping wires, batteries, and other electrical systems away from the user. This will allow for the mitigation of many of these safety concerns presented above. We found that with thus test sequence ethos will assist each time a individual wants to use the prostatic and not just during our testing faces of our device. We can also see that when looking at the risk trade off analysis our initial RPN is 80 however after implementing these mitigation features we are able to get this as low as a 16. Overall we can see that while our device does have two critical failure points both will be mitigated and delt with before ever reaching our customer biases.

6.2 Initial Prototyping

While designing and building our initial prototype, our team had been prioritizing simplification of the system, applying our current knowledge to the best of our abilities. Our first design iteration featured a large housing box, single shaft, bearing, and T-shaped adapter, as depicted in Figure 7 below:

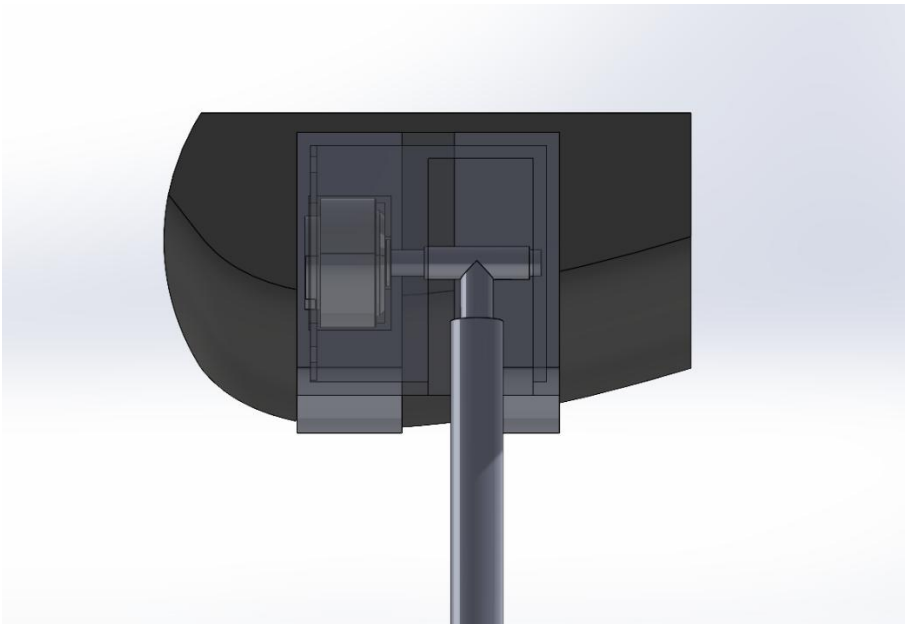

Figure 7: Initial Prototype Design

Further analysis of this design allowed us to take similar concepts and rework items that were no longer feasible, in which the following questions were answered:

What question are you trying to answer with the prototype?

With this design, our team was aiming to answer:

- Is this design practical and intuitive?
- Does this design facilitate movement in the sagittal plane?
- Is this design actively actuated?
- Is this manufacturable and user friendly?

What was the answer?

Building the physical prototype was extremely informative to our understanding and application, which revealed in various aspects what concepts worked, and what concepts needed to be redesigned. We found each question to be answered:

- Simple function does not imply practical function.
- The design is not intuitive or desirable, the system housing is extremely bulky and would protrude awkwardly for users.
- Movement is facilitated in the sagittal plane, but rotation is extremely far removed from the accurate hip center of rotation.

- The design is hard to assemble and manufacture, the housing is completely closed off except for the pylon clearance slot, which does not allow for components such as the motor to be assembled within it.

How did it inform design/how do you plan to iterate based on this new info?

Following the completion of this prototype design, our team collectively decided to reconsider the design for the prosthetic. In doing so, we adjusted design priorities, such as ease of assembly and user-friendly integration. Additionally, taking factors such as center of rotation closeness and weight distribution in account as well helped to inform us of how to move forward in the iterative design process and start of our redesign.

6.3 Re-design

Using our initial prototyping results, we found multiple possible problems within our design. To address these issues, we decided to review and then redesign parts of our prosthetics. Our new design uses a gear-based drive train with the motor attached at the leg that rotates around the center of rotation of the mechanism. Seen in figure 8 below, we can see that we use two spur gears powered along their respective shots and held together with a gear bearing combo. We proceeded forth, doing our calculations based on this design as we felt we would lean more towards this than our old design.

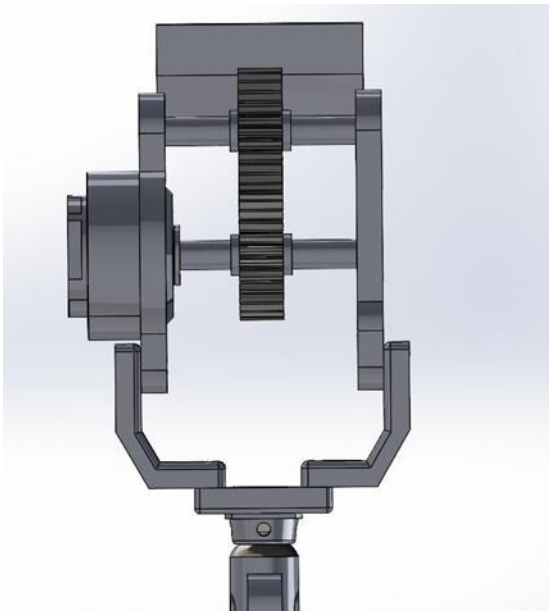

Figure 8: Current Prosthesis Design

6.4 Other Engineering Calculations

6.3.1 Structural Frame Analysis – Aiden Camisa

For structural frame analysis, I performed a stress calculation based on frames bearing wall thickness. In addition, I looked at the factor of safety of a variation of the lower bracket designs. Finally I confirmed everything by using a finite element analysis within SolidWorks on our models to test the stress and strength. Some of the assumptions we used for this calculation is that the body weight would be a 882.9N, with a reaction force of 1324 N. In addition, we would have a torsional motion of 120 N*m for the short-term movements within the motor itself on objects. In addition to these values, I used constants from aluminum 6061 T-1 and the sizing of our 3D model.

To perform these calculations, I used the equations below to allow for my calculations. In addition to the variables above, I used the thickness, lengths of certain pieces, and as well as diameters of the inside and outside frame portions around the bearings.

$$\sigma = \frac{M}{I} \qquad (27)\ M = F \cdot L \qquad (28)$$

$$I_{lower\ frame} = \frac{bt^3}{12} \qquad (29)$$

$$I_D = \frac{\pi(D_0 - D_i)}{64} \qquad (30)$$

$$FOS = \frac{\sigma_y}{\sigma} \qquad (31)$$

Using these equations, I am able to calculate the FOS for the bearings of 3.24 which is above our minimum of 2. This shows that the thickness of frames around the bearings will hold during stress. In addition to this I get a stress value of a newer design to only be 42.55MPa which is lower than our old design. This shows that while both beat the aluminum yield strength, the new design beats it by a significant margin compared to our old design. Finally, to help verify this info, I used the simulation software to look at the stress within the system.

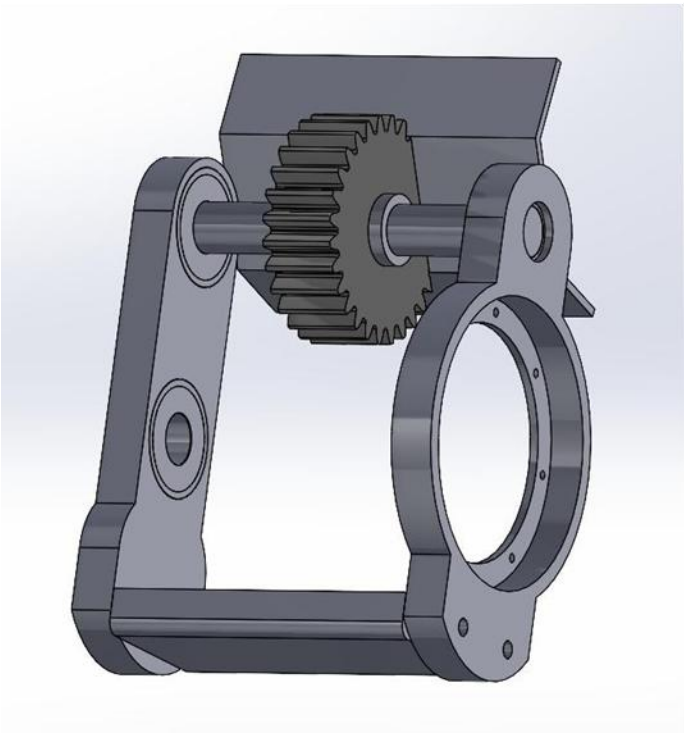

Figure 9: New Frame design Model

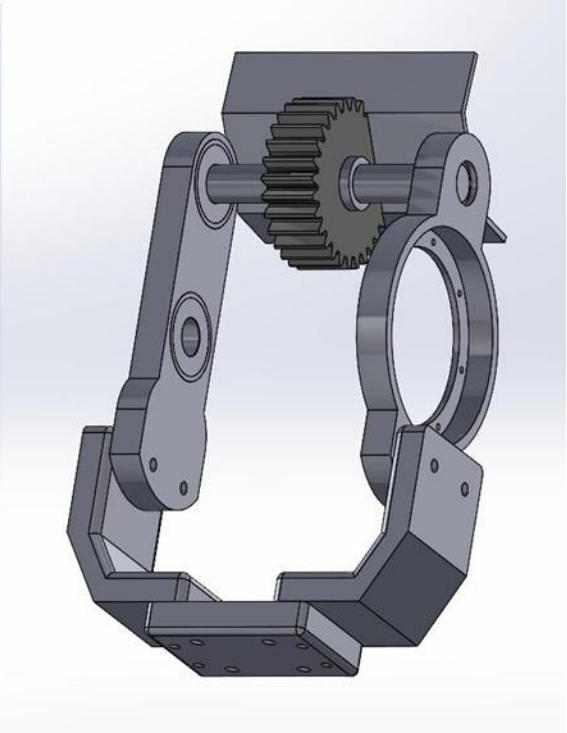

Figure 10: Current Frame design Model

Above we can see the current revisions of the frame with our potential new frame on the left and a older design on the right.

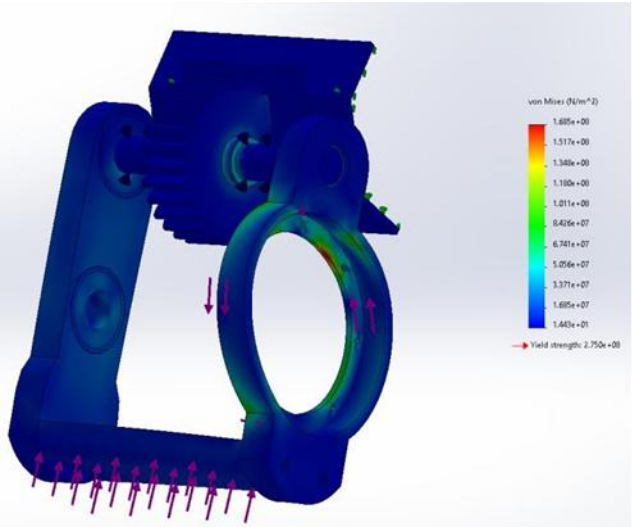

Figure 11: Stress for New design

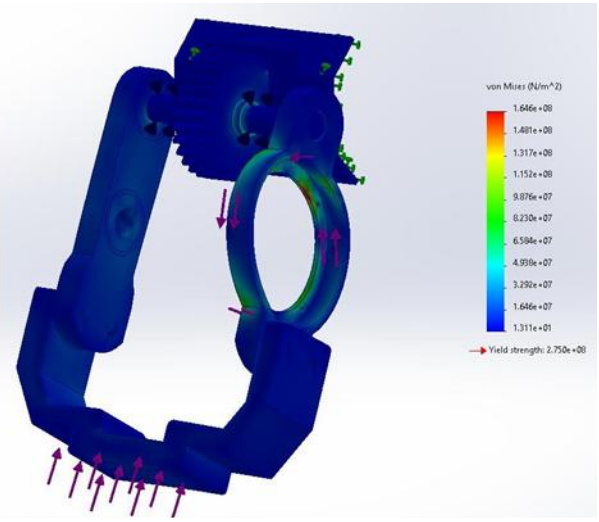

Figure 12: Stress for Current design

Above we can see just the stress variations of the SolidWorks simulation. A couple of interesting

things about these models is some of the increased load caused by the motor on the lower shaft on our old design with the newer design, we can see that it disappears. In addition to this we can see that the values are relatively small, showing that while there is difference the forces are not massive enough to cause great breaks within our system. Overall, we can see that the newer flatter design appears to work better so we will be proceeding forth with this design.

6.4.2 Battery Analysis – Quinn O'Neill

The team needs a battery to power the motor in order to lift the leg. This battery must be chosen based on if it allows the motor to produce enough power, and the energy stored by the battery is enough to allow the user to use the leg for long enough.

To start, we need to find the required voltage of the motor. To do this we found the required torque and rotational speed of the motor based on a study and dataset detailing the amount of torque at the hip for lifting the leg, and the rotational speed at which it is lifted [28]. Using the formula:

$$P = T \times \omega \tag{32}$$

Where P is power (Watts) T is torque (Nm) and ω is rotation speed (rad/s). Plugging the data and formula into MATLAB we got a graph that looks like this:

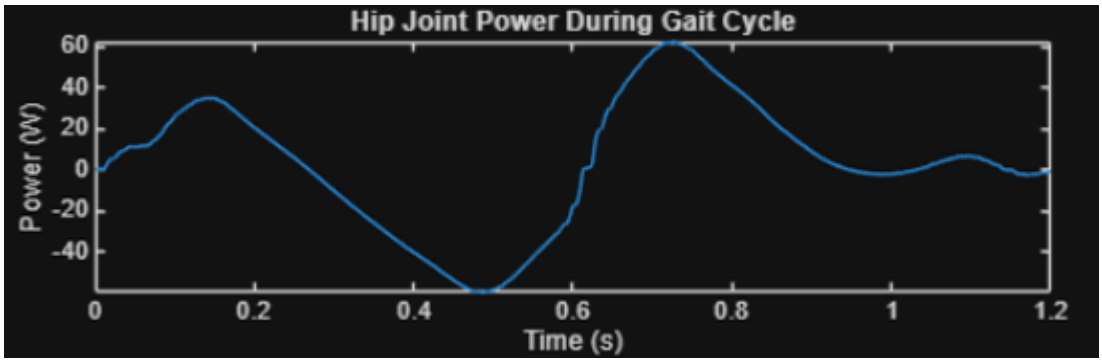

Figure 13: Hip joint power per gait time

From this data we get an average of 23.98 Watts per step. Then using listed data from our selected motor, the Cubemars AK8064 KV 80, we were able to find the required amperage per the gait cycle using this formula:

$$\mathrm{I} = T/kt \tag{33}$$

Where I is current (Amps), T is torque (Nm), kt is a rated torque constant (Nm/A). resulting in following:

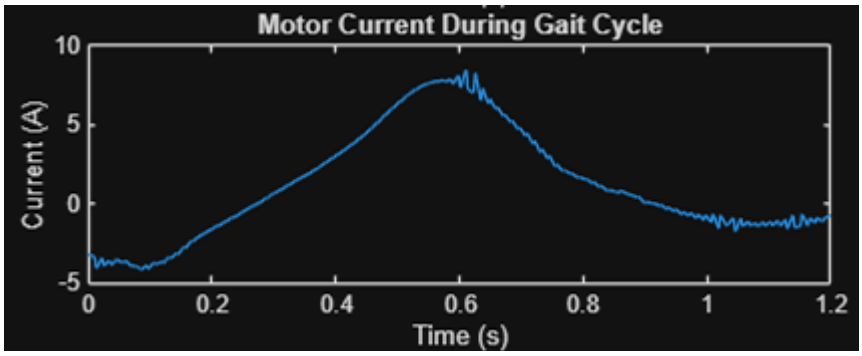

Figure 14: Motor current per gait time

Then doing a matrix division of the Power and the current results in the following graph, showing the voltage for the motor required.

$$V = P/I \tag{34}$$

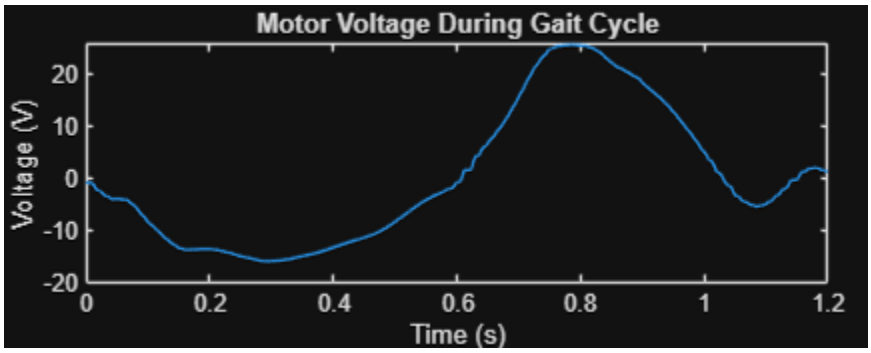

Figure 15: Motor Voltage per gait time

This graph gave us the Maximum motor voltage value of 25.7503 Volts. The motor is rated for Voltages of 12/24/36/48, meaning the minimum required input voltage for this to motor to function at its max efficiency is 36V.

Our next goal is to find how much energy we need for the users of our product to achieve what they want to and then find a battery with that Energy. First, we need to set a limit to our user's goal. We decided we wanted to allow our customers the recommended 10,000 steps a day for general fitness. Because we are only designing for 1 leg, we need to allow only 5000 per that leg, however since we want to allow our user to go above and beyond, and account for activity other than walking, we landed on an allowed 10,000 steps for our leg.

Taking the average power per step of 23.98 Watts and taking an average step time of 1.2s from our walking study [], we can determine the Energy used per step with the following formula:

$$E = P * t \tag{35}$$

Where E is energy (Joules) and t is time (seconds), resulting in a step energy of 28.78 J.

Multiplying by our desired step count of 10,000 we get a required energy of 287,800 Joules stored within the battery. Most batteries have a listed number of Amp-hours or Watt-hours. Watt hours are a form of energy stored in a battery per full charge. Amp-hours can easily be converted to Watt-hours by multiplying our chosen battery voltage. Converting our Energy to Watt hours requires the following conversion formula:

$$E(Wh) = \frac{E(j)}{60\left(\frac{min}{hr}\right)\times 60\left(\frac{s}{min}\right)} \tag{36}$$

Resulting in a required battery rating of 79.9 Wh or 2.22 Ah

From the required energy and voltage, the team searched for and was able to find a battery that met these requirements and a relatively lightweight compared to other 36 V batteries on the market

Figure 16: Selected battery for the team [38]

The selected battery has a rated voltage of 36V, capacitance of 4.4 Ah, and while this battery unfortunately has no listed weight, it has a listed dimensioning of $1.3 * 3.5 * 5.3\ in3$, significantly smaller than many 36 V batteries on the market.

6.4.3 Shaft and Bearing Analysis - Victoria

Building further upon previous shaft analysis, the updated design features two shafts that must support the gears, bearings, and properly transmit the required torque to enable hip rotation. Additionally, to assist in handling the load imposed by use, bearings will be utilized. To begin preliminary shaft design and bearing selection, it is necessary to note how the gears and bearings will be installed onto the shaft—the bottom shaft of the design is directly mounted to the motor and is fitted with a single bearing on the

opposite side in which the inner ring will be rotating. However, the upper shaft features bearings on both sides, and is to remain stationary, therefore the upper shaft bearings outer rings will rotate. As a result, a tight interference fit will be used to install the bearings to the shafts. The top shaft will require a tight inner ring, with a loose outer ring as the load rotates with it. Oppositely, the bottom shaft bearing will require a tight outer ring fit and loose inner ring fit. The interference for these installation types will be computed further in fabrication processes.

For shaft materials, it is recommended to use low carbon steel. With this in mind, a preliminary material of AISI 1050 CD is selected for both shafts. The steel has the following material properties:

$$S_{ut} = 690\ MPa$$
$$S_y = 580\ MPa$$

To determine the minimum diameter applicable, the following assumptions and parameters are defined:

- $90\ kg$ individual
- Due to oscillating movement in use, the bending stress is completely reversed.
  - $M_m = 0 = T_a$
- Gear face width, $F = 25.4\ mm$
- Shaft length, $L = 115\ mm$
- Maximum moment at the hip joint during flexion, $M_a = 98\ N * m$
- Maximum torque at the hip joint during gait, $T_m = 66\ N * m$, calculated in previous team analysis.
- Initial ratios of $\frac{D}{d} = 1.5, \frac{r}{d} = .02$ in regard to the variable diameter sizes and shoulder filets.
  - $K_f = K_t = 2.7$
  - $K_{fs} = K_{ts} = 2.2$
- Initial factor of safety, $n = 1$
- Desired reliability, $R = 0.99$

Note that many of these parameters are preliminary and will require further iteration with solidified dimensioning as a result of gear and bearing selections. To solve for the diameter size, the von Mises stress equation is rearranged:

$$d = \left(\frac{16n}{\pi}\left\{\frac{1}{S_e}\left[4\left(K_f M_a\right)^2\right]^{\frac{1}{2}} + \frac{1}{S_{ut}}\left[3\left(K_{fs} T_m\right)^2\right]^{\frac{1}{2}}\right\}\right)^{\frac{1}{3}} \quad (37)$$

Using these initial values, a diameter of $d = 23.14\ mm$ is computed, which is larger than the required shaft restriction. Further, based upon this result, the center diameter would measure $D = 34.71\ mm$, and notch radius of $r = 0.4628\ mm$. However, as a preliminary calculation, further iteration will be carried out in order to further reduce the diameter size as the dimension ratios were assumed to be worst case, as recommended in *Shigley's Mechanical Engineering Design.* To do so, we now compute actual K_f and K_{fs} values using the radius, and continue diameter iteration.

$$K_f = 1 + \frac{K_t - 1}{1 + \sqrt{a}/r} \quad (38)$$
$$K_{fs} = 1 + \frac{K_{ts} - 1}{1 + \sqrt{a}/r} \quad (39)$$

Where $\sqrt{a}$ is the Neuber constant based on material properties, defined for both bending and torsion:

$$\sqrt{a}_{bending} = 0.246 - 3.08(10^{-3}) \times S_{ut} + 1.51(10^{-5}) \times {S_{ut}}^2 - 2.67(10^{-8}) \times {S_{ut}}^3 \quad (40)$$
$$\sqrt{a}_{torsion} = 0.190 - 2.51(10^{-3}) \times S_{ut} + 1.35(10^{-5}) \times {S_{ut}}^2 - 2.67(10^{-8}) \times {S_{ut}}^3 \quad (41)$$

The updated values are input into a MATLAB iterative loop, computing the diameter until

convergence. Note that the converged diameter is still for initial ratios of $\frac{D}{d} = 1.5$ and $\frac{r}{d} = .02$, therefore the stress concentration factors remain as $K_t = 2.7$ and $K_{ts} = 2.2$. Future calculations can provide further accuracy and improved dimensions.

The final converged result yields a diameter of $d = 15.76\ mm$, leaving about $1.24\ mm$ until the maximum diameter restriction is reached. Therefore, the center diameter is $D = 23.64\ mm$, and notch radius $r = 0.3152\ mm$.

Based upon typical human gait, the team previously computed that the leg experiences about $1324\ N$ in ground-reaction forces, composed of $1244\ N$ which is radial, and $453\ N$ which is axial. Accounting for forces in both directions, an angular contact ball bearing will be selected. Using the computed shaft diameter as a guideline for bore specifications, we select an SKF 7202 BE angular contact ball bearing to support each shaft. This bearing has a dynamic load rating of $C_{10} = 39.3\ kN$ and static load rating of $C_0 = 21.4\ kN$, which is more than suffice for the current application forces.

Further, the shaft will require retaining rings by means of gear alignment, and a key and keyway in order to properly transmit the torque from the motor to the gear set. Given that the minimum center diameter is $D = 23.64\ mm$, we increase to $D = 25\ mm$ and select retaining ring DSR-25. This specific ring is external and thus housed directly on the shaft. This requires a groove diameter of $D_g = 23.9\ mm$, which allows for tolerance from the calculated minimum central diameter. The ring has load handling capabilities of $P_r = 45\ kN$ of thrust on the ring, and $P_g = 8.30\ kN$ of thrust on the groove, which is more than sufficient to withstand the defined thrust experienced in gait. Lastly, in designing a key for each shaft, *Shigley's Mechanical Engineering Design* includes a table in which typical shaft diameters and suitable key and keyway sizes are listed. Considering that this key will sit on the top center diameter, the table is assessed for a $25\ mm$ diameter shaft. A key of $w = 6.35\ mm$ and $h = 4.76\ mm$ and keyway depth of $2.38\ mm$ would be suitable for the shaft.

6.4.4 Gear Analysis - Matt

To support the ongoing development of the powered hip prosthesis, a detailed analysis of potential gearsets for the actuator assembly. The goal was to replace the placeholder gears in the current CAD model (Figure 9) with components that are mathematically justified, meet torque and power requirements, and minimize size while maximizing delivered torque. The new gearset must reliably transmit the peak torques observed during gait, operate with low noise/vibration, and fit the spatial constraints imposed by the motor and socket.

To establish constraints, the team assumed that the gear bore must be 0.75 in to accommodate the CubeMars AK80-64 motor shaft and fastener arrangement. Because the design uses parallel shafting, helical gears, if chosen, must be paired as left-hand and right-hand variants. The powered joint must safely transmit 66.2 N-m (585.92 lb-in) of torque, 0.084 horsepower, and rotational speeds up to 27.7 rpm during gait. MATLAB derived joint profiles Figures 3 and 4 showed gait to be the most demanding motion condition. A service factor of 1.25 was applied to account for uniform-to-moderate shock loading, increasing the minimum allowable transmitted torque to 732.4 lb-in.

Using equations and rating methods provided in Boston Gears' *Rotary Drive Products* catalog, the team evaluated spur gears at 14.5° and 20° pressure angles as well as helical gears at 14.5°. Catalog data for allowable torque, horsepower, diametral pitch, face width, and pitch diameter were used to compute gear volumes. Torque-per-volume (T/V) served as the key metric because minimizing component size while maximizing torque capacity is critical for packaging inside a prosthetic hip. Hardened steel gears were selected as the baseline material due to superior load capacity and favorable

strength-to-weight characteristics compared to bronze and cast iron. The equations used by Boston Gears are:

$$W = \frac{SFY}{P}\left(\frac{600}{600+V}\right) \quad (42)$$

$$T = \frac{W \times D}{2} \quad (43)$$

$$HP = \frac{WV}{33000} \quad (44)$$

Where allowable torque is T, power is HP, and allowable load is W. Also, SF is the safety factor, Y is tooth form factor, P is diametral pitch, V is pitch line velocity, and D is diameter. Equation 42 is for a spur gear. To calculate allowable load of a helical gear, diametral pitch is replaced with normal diametral pitch. Tooth form factors are based on number of teeth and are shown in the tables below:

Number of Teeth	14-1/2° Full Depth Involute	20° Full Depth Involute
10	0.176	0.201
11	0.192	0.226
12	0.210	0.245
13	0.223	0.264
14	0.236	0.276
15	0.245	0.289
16	0.255	0.295
17	0.264	0.302
18	0.270	0.308
19	0.277	0.314
20	0.283	0.320
22	0.292	0.330
24	0.302	0.337
26	0.308	0.344
28	0.314	0.352
30	0.318	0.358
32	0.322	0.364
34	0.325	0.370
36	0.329	0.377
38	0.332	0.383
40	0.336	0.389
45	0.340	0.399
50	0.346	0.408
55	0.352	0.415
60	0.355	0.421
65	0.358	0.425
70	0.360	0.429
75	0.361	0.433
80	0.363	0.436
90	0.366	0.442
100	0.368	0.446
150	0.375	0.458
200	0.378	0.463
300	0.382	0.471
Rack	0.390	0.484

Table 8: Y Factor for Spur Gears

FOR 14-1/2°PA—45° HELIX ANGLE GEAR			
No. of Teeth	Factor Y	No. of Teeth	Factor Y
8	.295	25	.361
9	.305	30	.364
10	.314	32	.365
12	.327	36	.367
15	.339	40	.370
16	.342	48	.372
18	.345	50	.373
20	.352	60	.374
24	.358	72	.377

Table 9: Y Factor for Helical Gears

Across all evaluated gearsets, the helical gears with 10 teeth in Table 12 produced the highest torque per unit volume. Two variants existed with face widths of 1.0 in and 1.25 in. The 1.25-in-wide option provides increased load capacity (948 lb-in allowable torque), comfortably above the 732.4 lb-in requirement with service factor applied. These gears also meet the 0.75-in bore requirement and have a compact 1.667-in pitch diameter suitable for integration in the hip assembly.

Teeth	Power (HP)	Torque (lb-in)	P (Teeth/in)	Face Width (in)	Diameter (in)	Volume (in^3)	Torque per Unit Volume (T/V)
25	.29	742	10	1	2.5	4.91	151.12
11	.38	946	6	1.5	1.83	3.95	239.49
16	.31	778	8	1.25	2	3.93	197.96

Table 10: Spur Gear Specifications with Pressure Angle of 14.5

Teeth	Power (HP)	Torque (lb-in)	P (Teeth/in)	Face Width (in)	Diameter (in)	Volume (in^3)	Torque per Unit Volume (T/V)
64	.31	779	16	.75	4	9.42	82.7
36	.37	928	12	1	3	7.07	131.26
20	.31	784	10	1.25	2	3.93	199.49
14	.35	890	8	1.5	1.75	3.61	246.54

Table 11: Spur Gear Specifications with Pressure Angle of 20

Teeth	Power (HP)	Torque (lb-in)	P – Normal P (Teeth/in)	Face Width (in)	Diameter (in)	Volume (in^3)	Torque per Unit

							Volume (T/V)
30	.32	818	10 – 14.14	.875	3	6.19	132.15
24	.34	862	8 – 11.31	.75	3	5.3	162.64
16	.29	740	8 – 11.31	1	2	3.14	235.67
10	.3	758	6 – 8.48	1	1.67	2.19	346.12
10	.38	948	6 – 8.48	1.25	1.67	2.74	345.99

Table 12: Helical Gear Specifications with Pressure Angle of 14.5

The selected gears correspond to Boston Gear part numbers H610R-18004 (right-hand) and H610L-18006 (left-hand). Figure 17 shows the catalog-listed configuration. Adopting this gearset enables the team to move confidently into Prototype 2 with a component that is load-justified, compact, and manufacturable. The next task for the team will be procurement and mechanical integration into the evolving CAD assembly.

Figure 17: Gear H610R Found on Power Motion and Industrial Supplies

6.5 Future Testing Potential

Once the full prototype is pieced together, the team will go through multiple testing processes through the second semester.

Test 1: the first of these tests will be testing our raspberry pi system to ensure it is able to turn the motor according to our inputs. The test will use our completed program in order to tell the motor when to turn, and with what angle and speed to turn at. This test will be completed before the end of the first semester.

Test 2: secondly, we test that the motor has enough power to lift the leg will start by loading or donated model leg to our fully motorized hip. With the controlled motor we will test if the motor is able to lift the leg, and if the rest of the model holds up without breaking and buckling. This will also test if the battery is able to power the motor reliably.

Test 3: Testing if the leg is capable of walking. This includes testing if the leg can handle the weight plus reaction force of walking. It also includes testing if it's able to balance and move comfortably and is best able to simulate walking with a sound leg. This test will require the team to create a bypass. This bypass will try to load the prosthetic as close to where it would be loaded on the theoretical user, however it will not be perfect as each of the team members used to test on both legs sound. The bypass still needs to be designed fully, but the team is already brainstorming ideas.

Test 4: Testing the leg in various situations such as jogging, walking up inclines, and standing up from sitting. This will look a lot like the testing done in the 3rd round of testing, just with more challenging parameters. This will also require the team to expand our motor control code.

Test 5: The team's ideal goal is to have the leg move automatically without manual inputs of the team. We will find and test a sensor system for the leg to know then to activate the motor and to deactivate the motor. The team does not yet have a sensor system but the plans we have so far are a motion sensor at the foot (which is straightforward but will have strange wiring to the motor), or a suspension weight sensor above the knee (trickier to design, but a more compact system).

7 CONCLUSIONS

This report summarizes the progress and outcomes of our semester-long effort to design an active, powered hip prosthesis for individuals with hip disarticulation amputations. Although these amputations account for only about 1% of all limb losses, they present some of the most severe mobility challenges.

Many individuals who undergo this procedure lose the ability to walk independently and are confined to wheelchairs due to the lack of effective prosthetic options. Existing hip prostheses are predominantly passive designs that rely heavily on the user's momentum and upper-body control. These systems often fail to provide adequate stability, energy efficiency, or assistance during tasks such as walking, climbing stairs, or rising from a seated position. The primary objective of our project has been to address these limitations by developing a powered hip prosthesis capable of restoring a greater degree of natural, energy-efficient mobility.

Throughout this semester, with the help of our project mentors, we've established clear customer and engineering requirements to guide our design process. Our clients/ sponsor mentors require a prosthesis that is stable, efficient, and comfortable to use. The design must provide a stable leg capable of supporting a user weighing up to 90 kg throughout all phases of gait, including stance, swing, and transitions such as standing or sitting. The prosthesis must enable natural walking and stair climbing, requiring a sufficient range of motion and power output from the actuator. We determined that a hip joint capable of achieving a range of –30° to 100° of motion relative to the neutral standing position would best replicate the necessary gait cycle. Further, the motor supplying power must provide a minimum torque of 22N-m.

Our team's collaboration with Next Step Prosthetics and participation in the NSF I-Corps Aspire Course have been incredible assets for both the technical and financial aspects of the project. Through NSF I-Corps, we have gained insight into customer discovery and evaluation, which has been useful for gaining lots of differing insights to inform our design, as well as many networking opportunities for future potential sponsorships. Further, in working closely with Next Step Prosthetics, we have gained invaluable access to materials, knowledge and mentorship, tools and workspaces, and direct contact with a hip disarticulation patient. The combined financial and material support—totaling approximately $8,000 in funding and resources—positions our team exceedingly well, and we are confident to continue our design and developmental processes.

To assess design criteria and development, a mathematical model was developed, assessing criteria ranging from static force assessments to motor torque and power requirements.

The final proposed solution is a single-plane powered hip prosthesis designed to operate primarily in the sagittal plane, which corresponds to the natural forward and backward motion of the leg during walking. By focusing on a single degree of powered motion, the design minimizes unnecessary weight and complexity while maximizing performance for high-demand tasks such as walking, stair ascent, and transitioning from sitting to standing. The final electrically actuated system will include a sensor-driven control system as well, to help create a customizable gait for natural cycles and improve system adoption.

8 References

[1] “AK80-64 KV80 Robotic Actuator - 64:1 Ratio, 120Nm Peak Torque,” CubeMars, 2025. https://www.cubemars.com/product/ak80-64-kv80-robotic-actuator.html

[2] “Ottobock,” Ottobock, 2025. *Helix3D prosthetic hip joint | Helix3D prosthesis solution* (accessed Sep. 15, 2025).

[3] “Modular Single Axis Hip Joint | Hips | Lower Limb Prosthetics | Prosthetics | Ottobock CA Shop,” *Ottobock.ca*, 2021. Available: https://shop.ottobock.ca/en/Prosthetics/Lower-Limb-Prosthetics/Hips/Modular-Single-Axis-Hip-Joint/p/7E5~5R

[4] H. J. Bennett, K. Fleenor, and J. T. Weinhandl, “A normative database of hip and knee joint biomechanics during dynamic tasks using anatomical regression prediction methods,” *Journal of Biomechanics*, vol. 81, pp. 122–131, Nov. 2018, doi:10.1016/j.jbiomech.2018.10.003.

[5] H. J. Bennett, K. Fleenor, and J. T. Weinhandl, “A normative database of hip and knee joint biomechanics during dynamic tasks using anatomical regression prediction methods,” *Journal of Biomechanics*, vol. 81, pp. 122–131, Nov. 2018, doi:10.1016/j.jbiomech.2018.10.003.

[6] E. D. Lemaire, T. J. Supan, and M. Ortiz, “Global standards for prosthetics and orthotics,” *Canadian Prosthetics & Orthotics Journal*, Oct. 2018, doi:10.33137/cpoj.v1i2.31371.

[7] G. G. Polkowski and J. C. Clohisy, “Hip biomechanics,” *Sports Medicine and Arthroscopy Review*, vol. 18, no. 2, pp. 56–62, Jun. 2010, doi:10.1097/JSA.0b013e3181dc5774.

[8] S. Au and H. Herr, “Powered ankle-foot prosthesis,” *IEEE Robotics & Automation Magazine*, vol. 15, no. 3, pp. 52–59, Sep. 2008, doi:10.1109/MRA.2008.927697.

[9] Y. Tian, A. Plummer, P. Iravani, J. Bhatti, S. Zahedi, and D. Moser, “The design, control, and testing of an integrated electrohydrostatic powered ankle prosthesis,” *IEEE/ASME Transactions on Mechatronics*, vol. 24, no. 3, pp. 1011–1022, Jun. 2019, doi:10.1109/TMECH.2019.2911685.

[10] R. Gehlhar, M. Tucker, A. J. Young, and A. D. Ames, “A review of current state-of-the-art control methods for lower-limb powered prostheses,” *Annual Reviews in Control*, Apr. 2023, doi:10.1016/j.arcontrol.2023.03.003.

[11] G. Stark, “Overview of hip disarticulation prostheses,” *Journal of Prosthetics and Orthotics*, LWW, 2025. [Online]. Available: https://journals.lww.com/jpojournal/fulltext/2001/06000/Overview_of_Hip_Disarticulation_Prostheses.14.aspx. [Accessed: Sep. 18, 2025].

[12] E. Gailledrat *et al.*, “Does the new Helix 3D hip joint improve walking of hip disarticulated amputees?,” *Annals of Physical and Rehabilitation Medicine*, vol. 56, no. 5, pp. 411–418, Jul. 2013, doi:10.1016/j.rehab.2013.05.001.

[13] F. Golshan, N. Baddour, H. Gholizadeh, and E. D. Lemaire, “A pelvic kinematic approach for calculating hip angles for active hip disarticulation prosthesis control,” *Journal of Neuroengineering and Rehabilitation*, vol. 20, no. 1, Nov. 2023, doi:10.1186/s12984-023-01273-x. [Online]. Available: https://www.ncbi.nlm.nih.gov/pmc/articles/PMC10634065/.

[14] M. Nietert, N. Englisch, P. Kreil, and G. Alba-Lopez, “Loads in hip disarticulation prostheses during normal daily use,” *Prosthetics and Orthotics International*, vol. 22, no. 3, pp. 199–215, Dec. 1998, doi:10.3109/03093649809164485.

[15] S. Mroz, N. Baddour, P. Dumond, and E. D. Lemaire, “Design and prototype validation of a laterally mounted powered hip joint prosthesis,” *Journal of Rehabilitation and Assistive Technologies Engineering*, vol. 11, Jan. 2024, doi:10.1177/20556683241248584.

[16] T. Chin, S. Sawamura, R. Shiba, H. Oyabu, Y. Nagakura, and A. Nakagawa, “Energy expenditure during walking in amputees after disarticulation of the hip: A microprocessor-controlled swing-phase control knee versus a mechanical-controlled stance-phase control knee,” *The Journal of Bone and Joint Surgery. British Volume*, vol. 87, no. 1, pp. 117–119, Jan. 2005.

[17] M. Botros, H. Gholizadeh, F. Golshan, D. Langlois, N. Baddour, and E. D. Lemaire, “Development of a powered four-bar prosthetic hip joint prototype,” *Prosthesis*, vol. 7, p. 105, 2025, doi: 10.3390/prosthesis7050105.

[18] M. S. H. Bhuiyan, I. A. Choudhury, M. Dahari, Y. Nukman, and S. Z. Dawal, “An investigation into a gear-based knee joint designed for lower limb prosthesis,” *Applied Bionics and Biomechanics*, vol. 2017, Art. no. 7595642, 2017, doi: 10.1155/2017/7595642.

[19] G. Giarmatzis, I. Jonkers, M. Wesseling, S. V. Rossom, and S. Verschueren, “Loading of hip measured by hip contact forces at different speeds of walking and running,” *Journal of Bone and Mineral Research*, vol. 30, no. 8, pp. 1431–1440, 2015, doi: 10.1002/jbmr.2483

[20] P. R. Golyski, B. K. Potter, J. A. Forsberg, and B. D. Hendershot, “Comparing the Mechanical Energetics of Walking Among Individuals with Unilateral Transfemoral Limb Loss Using Socket and Osseointegrated Prosthetic Interfaces,” *Scientific Reports*, vol. 15, no. 1, Art. no. 9755, 2025, doi: 10.1038/s41598-025-93211-1.

[21] T. Kawaguchi, T. Yamada, and K. Iwashita, “Biomechanical gait analysis for a hip disarticulation prosthesis: power source for the swing phase of a hip disarticulation prosthetic limb,” *Journal of Physical Therapy Science*, vol. 35, no. 5, pp. 361–365, 2023, doi:10.1589/jpts.35.361.

[22] X. Li, Z. Deng, Q. Meng, S. Bai, W. Chen, and H. Yu, “Design and optimization of a hip disarticulation prosthesis using the remote center of motion mechanism,” *Technology and Health Care*, pp. 1–13, Jun. 2020, doi:10.3233/THC-192088.

[23] P. P. Bonato, *Wearable Robotics: Challenges and Opportunities*, Springer, 2018.

[24] American Gear Manufacturers Association (AGMA), “Standards & Emerging Technology,” *AGMA.org*, 2025. [Online]. Available: https://www.agma.org/standards-technology/. [Accessed: Sep. 18, 2025].

[25] K. B. Fite, “Overview of the components used in active and passive lower-limb prosthetic devices,” in *Full Stride*, V. Tepe and C. Peterson, Eds., Springer, 2017, doi:10.1007/978-1-4939-7247-0_4.

[26] S. M. Zaffer, R. L. Braddom, A. Conti, J. C. Goff, and D. C. Bokma, “Total hip disarticulation prosthesis with suction socket: Report of two cases,” *American Journal of Physical Medicine & Rehabilitation*, vol. 78, no. 2, pp. 160–162, Mar. 1999.

[27] F. A. Gottschalk and M. Stills, “The biomechanics of trans-femoral amputation,” *Prosthetics and Orthotics International*, vol. 18, no. 1, pp. 12–17, Apr. 1994, doi:10.3109/03093649409164665.

[28] G. Bovi, M. Rabuffetti, P. Mazzoleni, and M. Ferrarin, “A multiple-task gait analysis approach: Kinematic, kinetic and EMG reference data for healthy young and adult subjects,” *Gait & Posture*, vol. 33, no. 1, pp. 6–13, 2011, doi:10.1016/j.gaitpost.2010.08.009.

[29] A. J. Young and D. P. Ferris, “State of the art and future directions for lower limb robotic exoskeletons,” *IEEE Transactions on Neural Systems and Rehabilitation Engineering*, vol. 25, no. 2, pp. 171–182, Feb. 2017, doi:10.1109/TNSRE.2016.2521160.

[30] D. E. Geiger, F. Behrendt, and C. Schuster-Amft, “EMG muscle activation pattern of four lower extremity muscles during stair climbing, motor imagery, and robot-assisted stepping: a cross-sectional study in healthy individuals,” *BioMed Research International*, vol. 2019, pp. 1–8, Mar. 2019, doi:10.1155/2019/9351689.

[31] L. Guo *et al.*, “On the design evolution of hip implants: A review,” *Materials & Design*, vol. 216, no. 110552, Apr. 2022, doi:10.1016/j.matdes.2022.110552.

[32] D. Dalli, J. Buhagiar, P. Mollicone, and P. Schembri Wismayer, “A novel hip joint prosthesis with uni-directional articulations for reduced wear,” *Journal of the Mechanical Behavior of Biomedical Materials*, vol. 127, p. 105072, Mar. 2022, doi:10.1016/j.jmbbm.2021.105072.

[33] J. Nilsson and A. Thorstensson, “Ground reaction forces at different speeds of human walking and running,” *Acta Physiologica Scandinavica*, vol. 136, no. 2, pp. 217–227, Jun. 1989,

doi:10.1111/j.1748-1716.1989.tb08655.x.

[34] “Shijiazhuang Perfect Prosthetic Manufacture Co., Ltd.,” *Shijiazhuang Perfect Prosthetic Manufacture Co., Ltd.*, 2025. [Online]. Available: https://www.sjzpfc.com/product-square-adapter-with-pyramid.html.

[35] A. Kharb, V. Saini, Y. K. Jain, and S. Dhiman, “A review of gait cycle and its parameters,” *ResearchGate*, Jan. 2011. [Online]. Available: https://www.researchgate.net/publication/268423123_A_review_of_gait_cycle_and_its_parameters.

[36] Boston Gear, *Boston Gear Product Catalog P-1930-BG*. Quincy, MA: Boston Gear, 2019. Accessed: Nov. 22, 2025.

[37] Boston Gear, “H610R Steel Helical Gear,” *Power Motion & Industrial Supplies*, Yakima, WA, USA. Available: https://pmisupplies.com/products/h610r-boston?srsltid=AfmBOopTI6H_BglRNie6a6LBGJJbulZuWcMDOuiC0LYGearGSgnZurqY. [Accessed: Nov. 22, 2025].

[38] Not a possible IEEE citation, but a link to the listed battery https://www.amazon.com/DFTIM-36V-Replacement-Hoverboard Configuration/dp/B0F5QF3Y23/ref=sr_1_5?crid=IQO7KYW02MEB&dib=eyJ2IjoiMSJ9.mxMr7FHO7IMqOHCSJy5VPTxZ0WjO3viewHjy3QOkU3qrnKXXt4MPlgI8cfwvCxQ4fT0FQ0C0EzZfD4BeuRpOGpN26xSLthMM9HEPJ9fdQCnErK4Hic0wXtnKeb29wYheQ7e34i5coKst97G6_yIQkfYZXsgrtIdVHhh93kQUhO91gzsV1qt-F93GMlWivNXuLQwSnry4N6luHVD2T6j13oGPIuJbTg_SE5HdfEdlVKA51ugEebFyPruLTlfc1JS5Tjorj10SPv2V7SMnd1ejcCQGrpzgrh0YaO8XQxE.rn3BmjKa95FjgpdARbP2H4pOy7C4KeKi6aDDHs5QxI8&dib_tag=se&keywords=36v+4400mah+battery&qid=1763873497&sprefix=36V+44%2Caps%2C118&sr=8-5

9 APPENDICES

9.1 Appendix A: Motor Analysis MATLAB Program

```
BW = 90;
torque = -BW*bovi.adult.normal.hip.sagittal.torque(:,2);
rms(torque) % for hip joint for continuous / gear ratio
position = bovi.adult.normal.hip.sagittal.position(:,2);
stride_time = 1.2;
time = linspace(0, stride_time, length(torque));
close all
subplot(311); plot(time,torque); % Flexion
subplot(312); plot(time,position); % Extension
subplot(313); plot(position, torque);
pos_rad = deg2rad(position);
vel_rad = dfdx(time,pos_rad);
acc_rad = dfdx(time,vel_rad);
close all
subplot(211); plot(time, vel_rad)
subplot(212);plot(time, vel_rad.*torque)
GR = 15;
motor_inertia = 579/10^7;
kt = .09;
R = .160;
vel_motor = vel_rad*GR;
tor_motor_static = torque/GR;
tor_motor_dynamic = motor_inertia*acc_rad*GR;
current = (tor_motor_static + tor_motor_dynamic)/kt;
volts = current*R + kt*vel_motor;
close all;
subplot(3,1,1); plot(time, volts);
subplot(3,1,2); plot(time, current);
subplot(3,1,3); plot(time, volts.*current)
close all;
% speed torque curve
plot(abs(current*kt), abs(vel_motor)); ylabel("motor speed rad/s"); xlabel("Motor
Torque Nm"); hold on;
w_limit = [570, 0]*2*pi/60;
t_limt = [0, 22];
plot(t_limt, w_limit, 'k'); hold off
GR = 25:45;
motor_inertia = 579/10^7;
kt = .09;
```

```
R = .160;
vel_motor = vel_rad.*GR;
tor_motor_static = torque./GR;
tor_motor_dynamic = motor_inertia.*acc_rad.*GR;

current = (tor_motor_static + tor_motor_dynamic)./kt;
volts = current.*R + kt.*vel_motor;
e_power = current.*volts;

i_max = max(abs(current));
i_rms = rms(current);
v_max = max(abs(volts));
p_max = max(abs(e_power));

close all;
subplot(411); plot(GR, i_max); ylabel("Amps"); hold on; yline(28); % peak current
limit
subplot(412); plot(GR, i_rms); ylabel("Amps"); hold on; yline(12); % continuous
current limit
subplot(413); plot(GR, v_max); ylabel("Volts"); hold on; yline(48); % votlage
limit
subplot(414); plot(GR, p_max); ylabel("Power");
```